

Latest ATLAS results on $H \rightarrow bb$ decays and Interpretation of Combined Higgs Measurements


Matt Klein (University of Michigan) on behalf of
the ATLAS Collaboration

2020 November 3




Recent $H \rightarrow bb$ History

- $H \rightarrow bb$ observed by ATLAS and CMS in 2018, mostly with $V(\text{lep})H(bb)$
- $H \rightarrow bb$ and VH measurements performed with unprecedented precision with the full Run 2 dataset - see LHC [seminar](#) in April



Recent Higgs boson property measurements with the ATLAS experiment

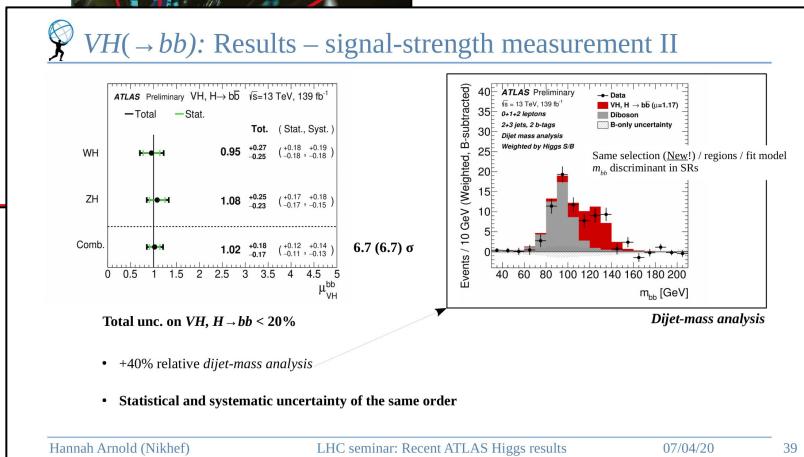
Hannah Arnold (Nikhef)
on behalf of the ATLAS Collaboration



LHC Seminar (CERN)
April 7, 2020

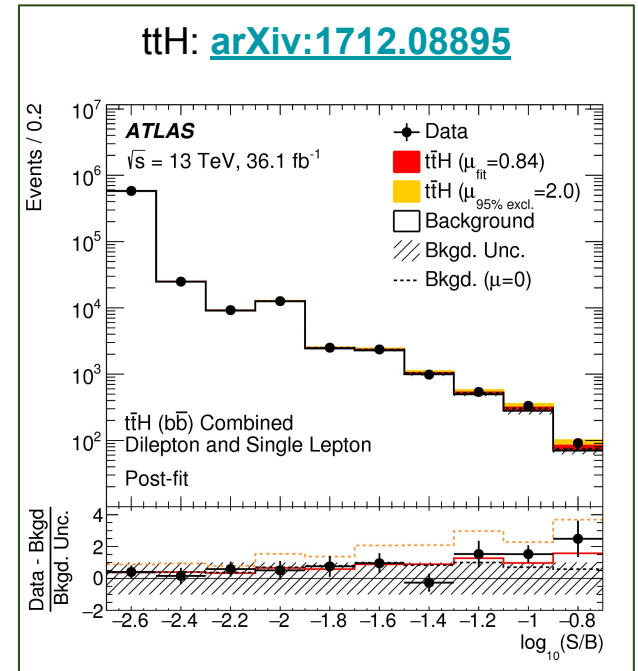
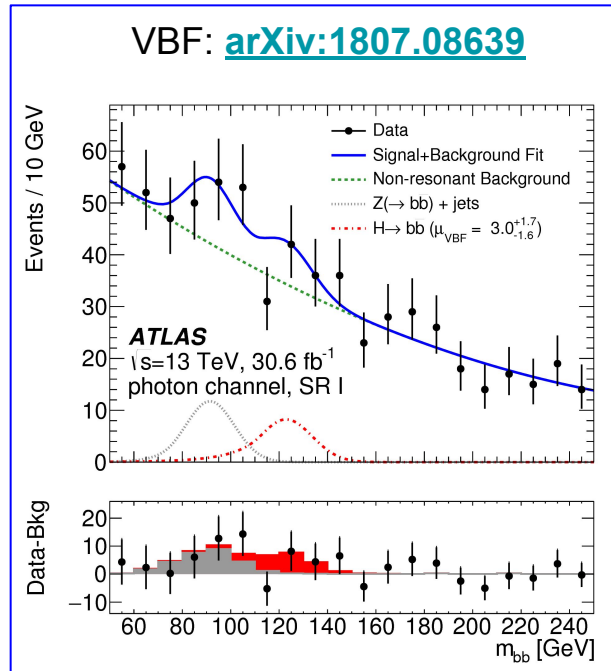
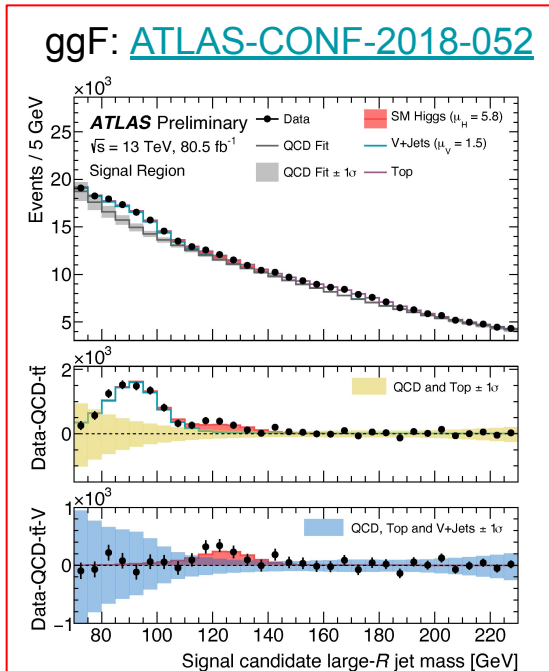


VH is the most sensitive $H \rightarrow bb$ production mode
 \rightarrow *Relatively* high signal relative to background
 \rightarrow Relative ease to trigger

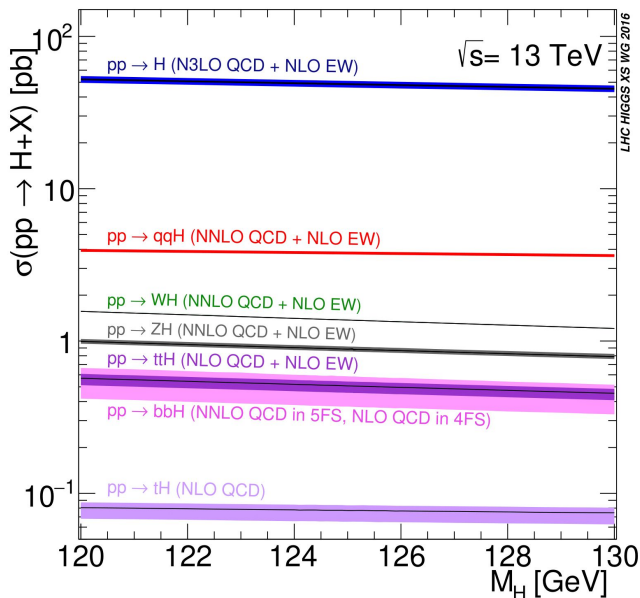


H→bb History

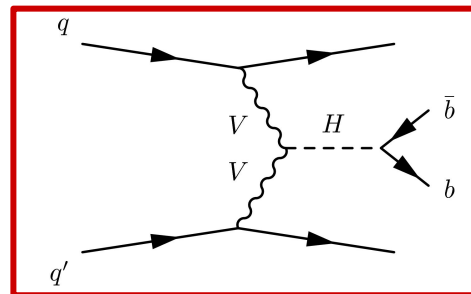
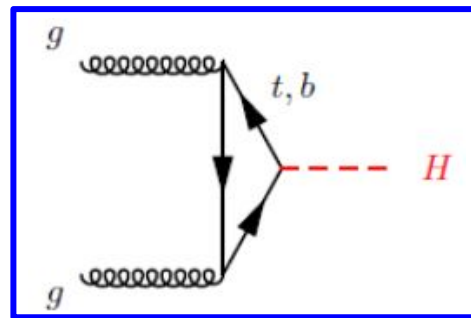
- **However** - VH is not the only production mode
- Other production modes allow for increased precision of Higgs coupling measurements, Higgs measurements at high p_T , and H→bb measurement not explicitly correlated with VH



Higgs Production Modes

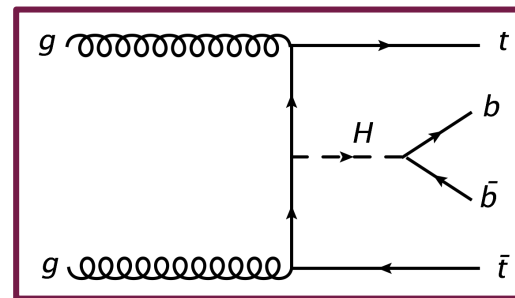
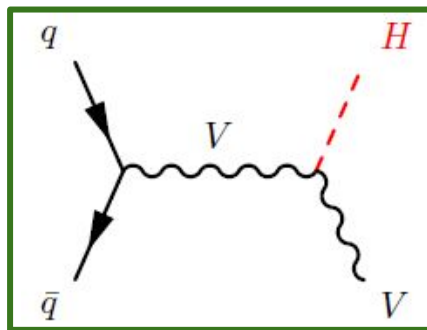


Expect $H \rightarrow bb$ 58% of time



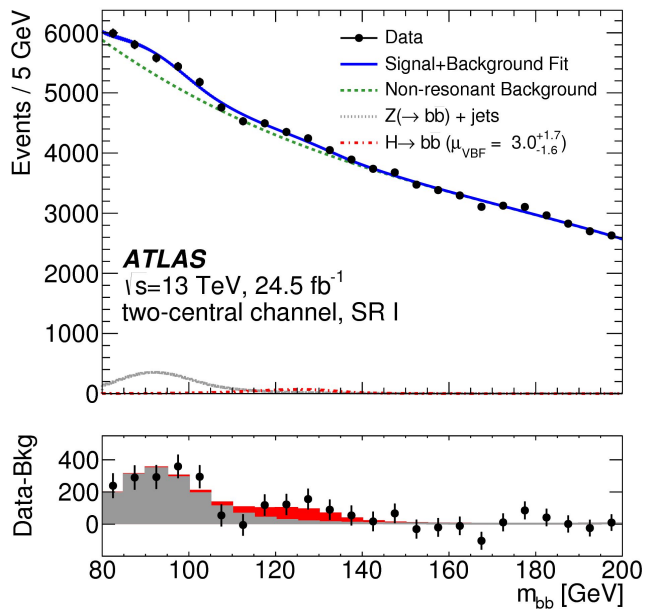
Decreasing cross-section

Decreasing background



History: VBF Hbb and VBF Hbb+ γ

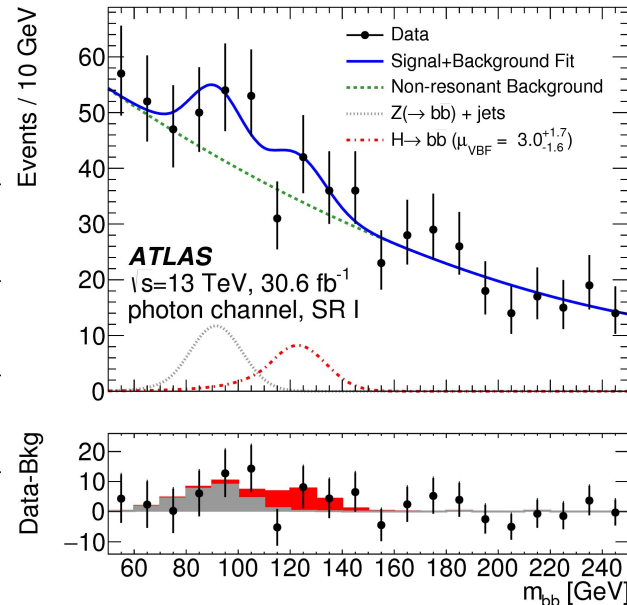
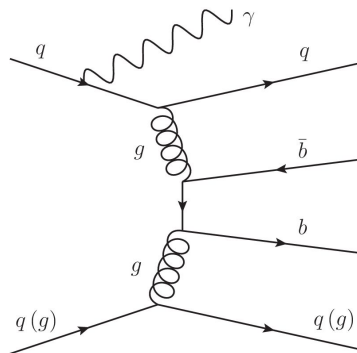
Large, difficult to model multijet background
 Smaller, peaked $Z \rightarrow bb$ background near signal
 Trigger on jets



Larger $Z \rightarrow bb$ background

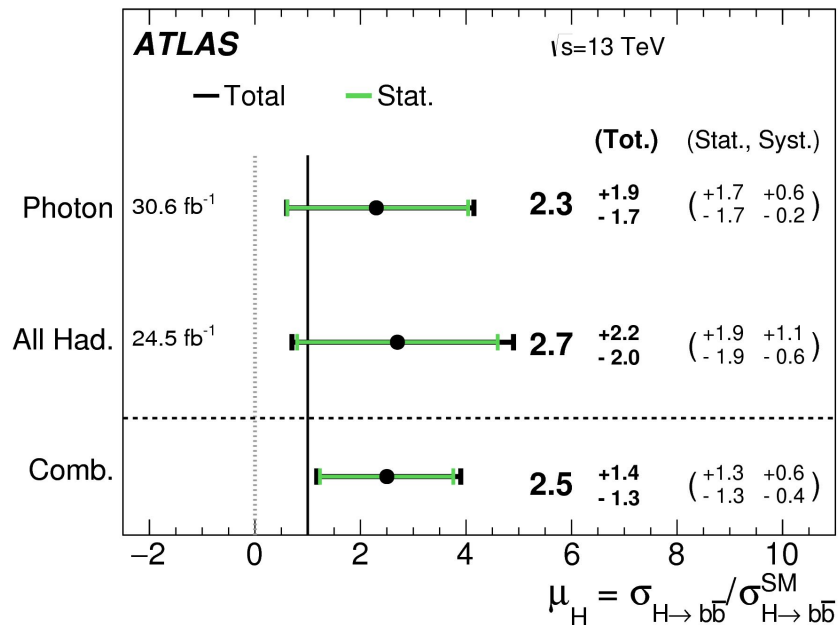
Mainly γ +jets background - gg-initiated diagrams suppressed

Trigger on γ +jets



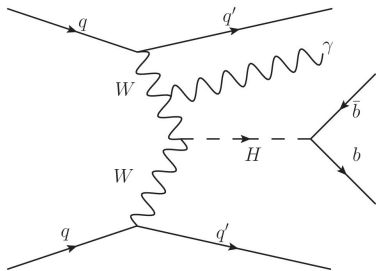
History: VBF $H \rightarrow b\bar{b}$

Results	Inclusive production		
	<i>All-hadronic</i>	<i>Photon</i>	Combined
Expected significance	0.5σ	0.6σ	0.8σ
Observed significance	1.4σ	1.3σ	1.9σ

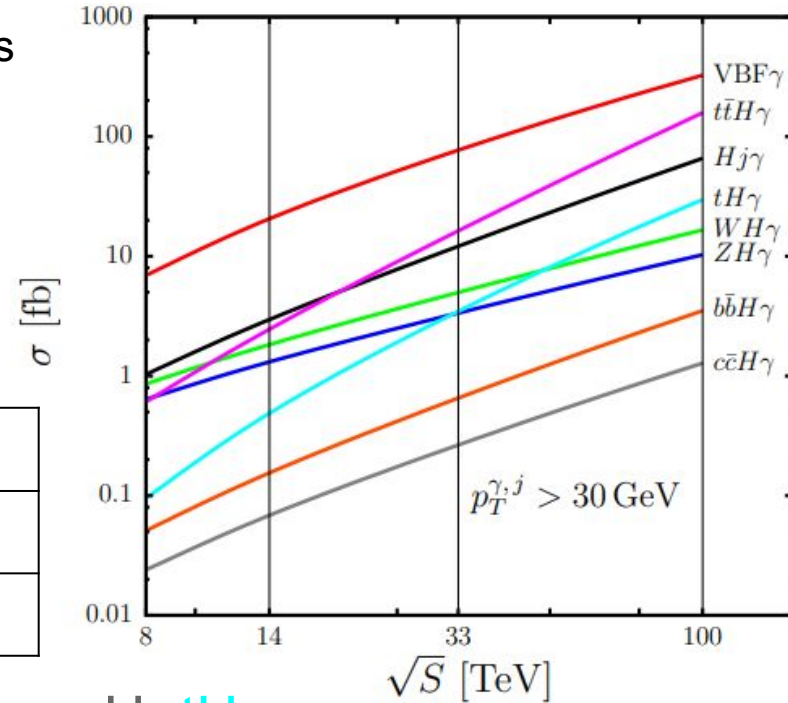


VBF+ γ

- γ decreases cross-section, but dramatically increases VBF yield relative to background
- γ from internal W: sizeable cross-section
- Enriched WW fusion compared to ZZ fusion



	Inclusive	+ γ (LO, 30 GeV)
ggF	49 pb	3 fb
VBF	3.8 pb	19 fb

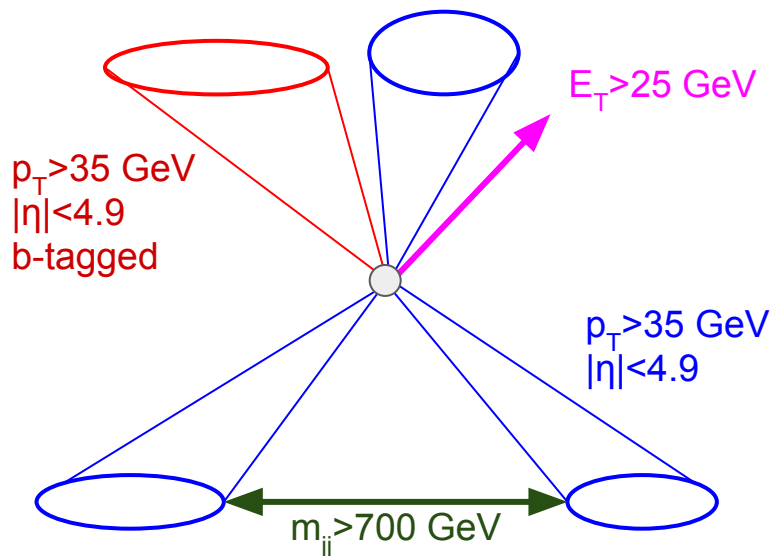


Without γ : ggF >> VBF > WH > ZH > ttH ~ bbH >> ccH ~ tH

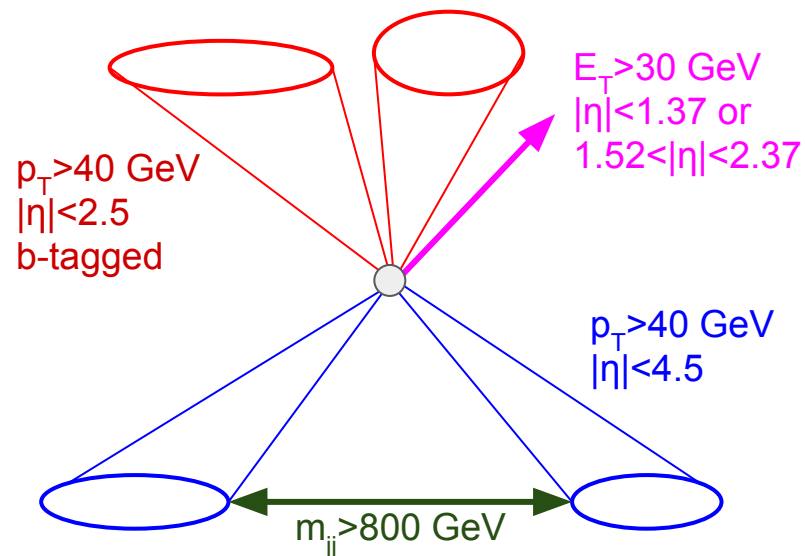
With γ : VBF >> ggF > ttH > WH > ZH > tH > bbH > ccH
at 13 TeV

VBF+ γ : Event Selection

Trigger (HLT) Selection



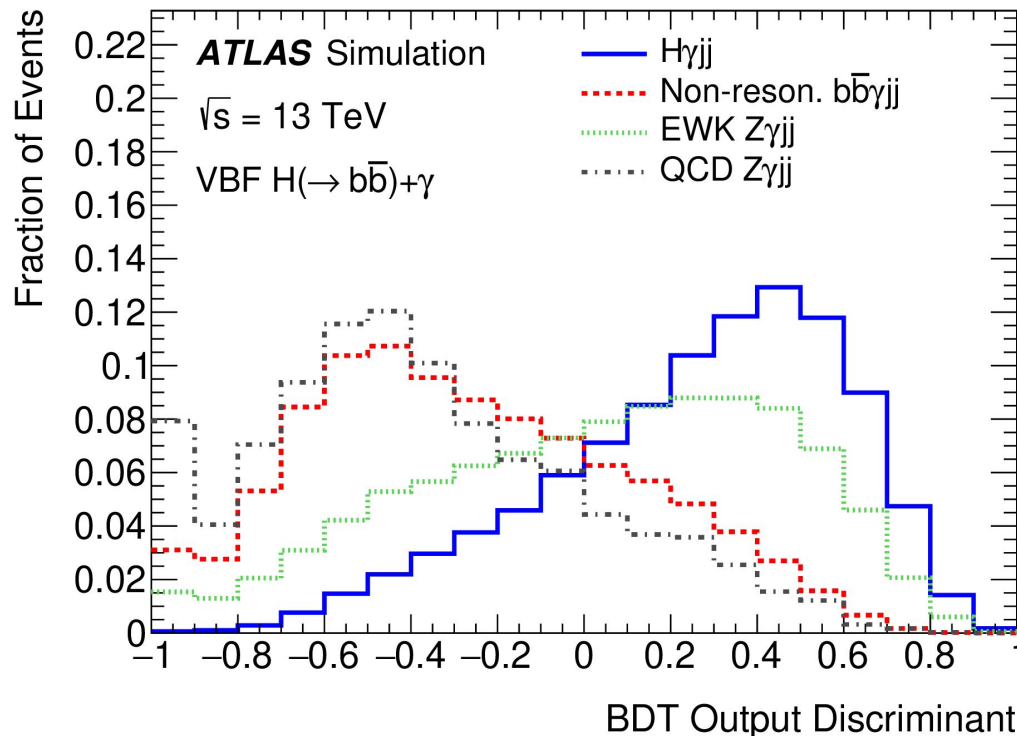
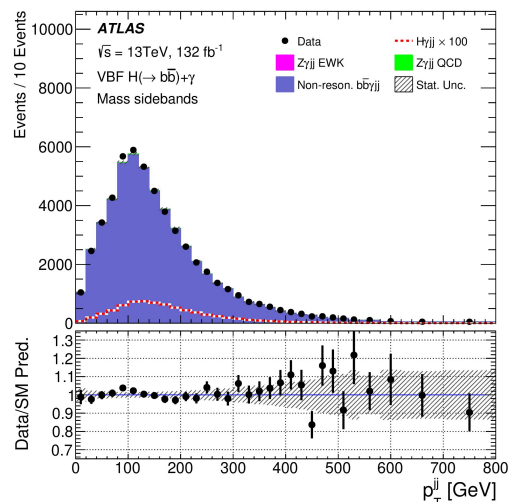
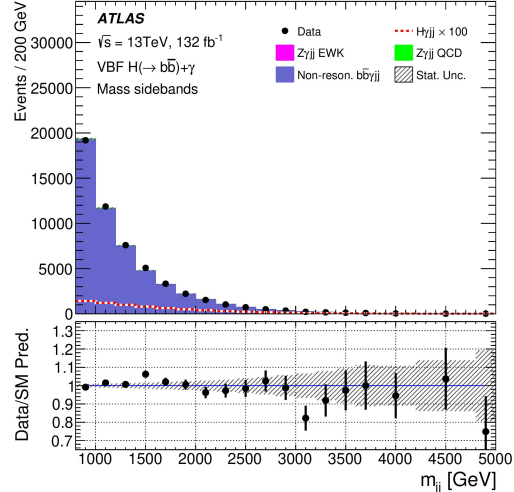
Offline Selection



Categorization

Train BDT to discriminate signal and background

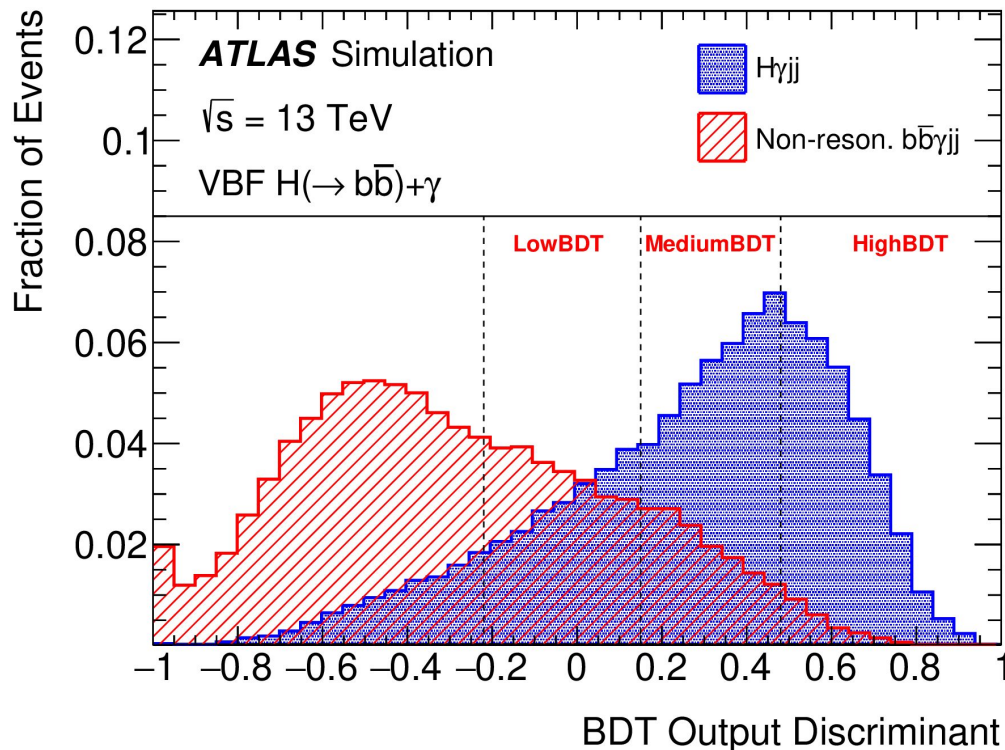
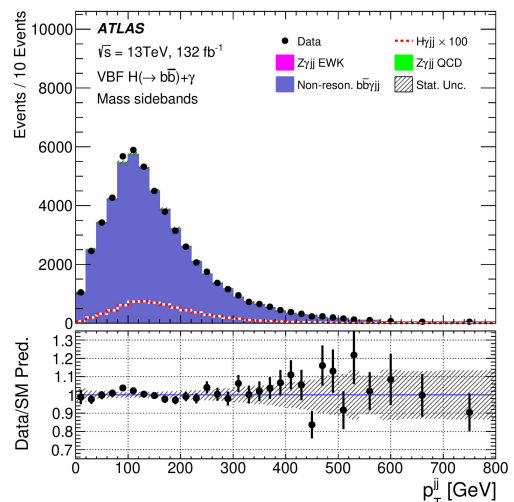
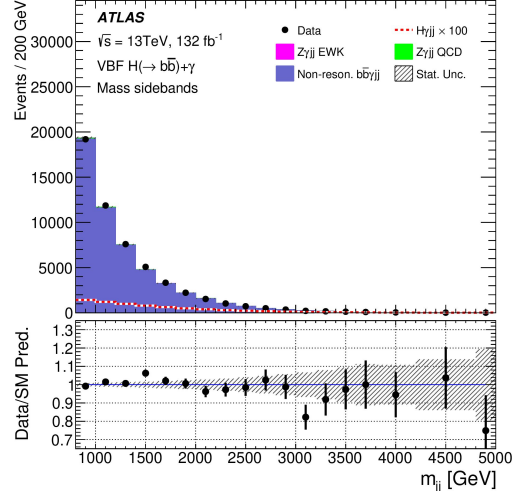
Exclude variables m_{bb} -correlated, to avoid sculpting background



Categorization

Categorize based on score, maximizing combined significance

Fit m_{bb} distribution in each region



Model and Spurious Signal

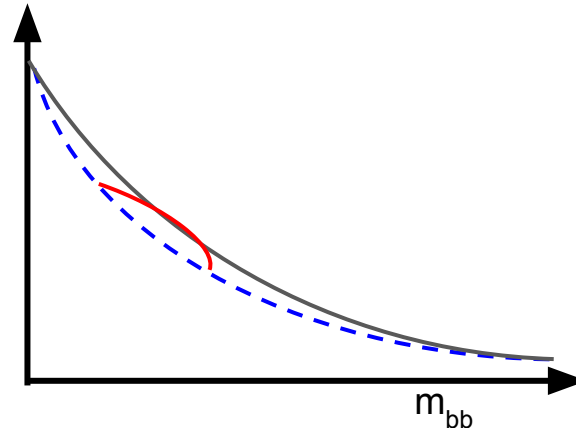
Fit data as sum of polynomial term (for non-resonant background) and peaks (Z and H)

1st order polynomial used in highest score region; 2nd order used in other regions

Primary systematic uncertainty is spurious signal - measures the potential inability of the background fit function to correctly fit the continuous background in data

Fit functions chosen to maximize sensitivity, subject to requirements on spurious signal uncertainties

Spurious signal estimated by fitting signal+background to large simulated background samples

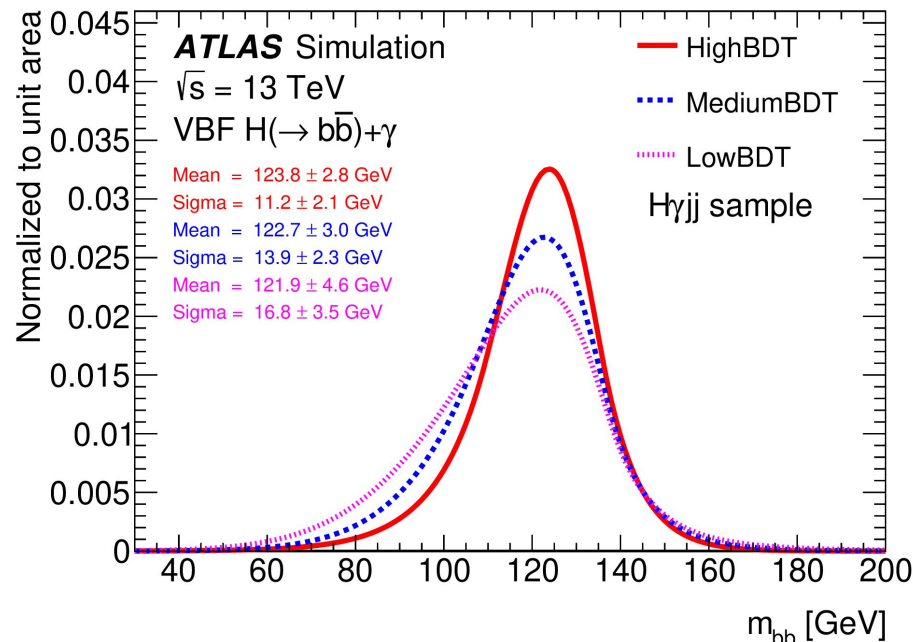
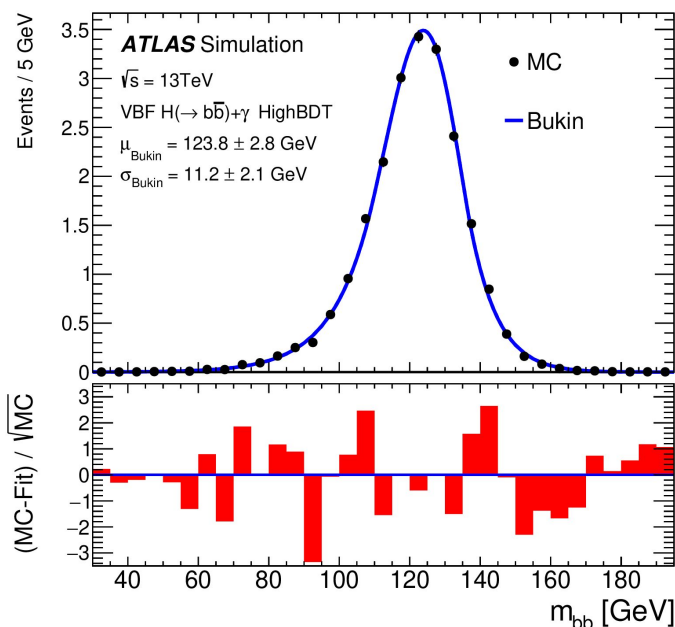


Signal and Fits

Uses b-jet energy corrections, derived in $VH \rightarrow bb$

Signal fit of m_{bb} distribution

Parameterize Z and H with Bukin functions

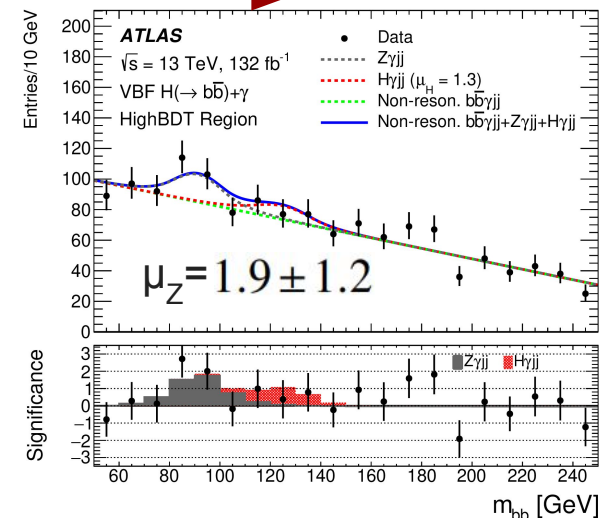
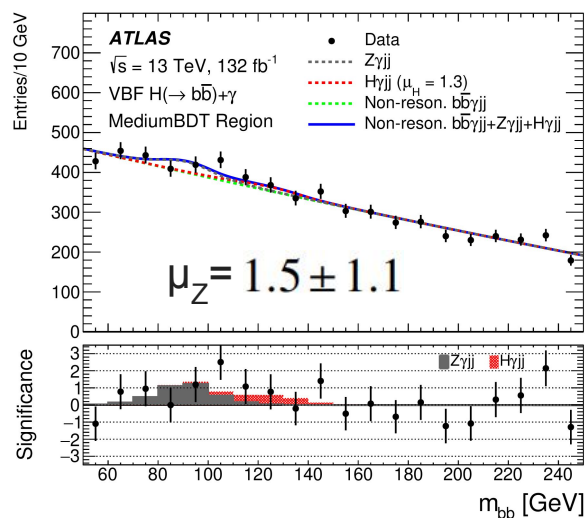
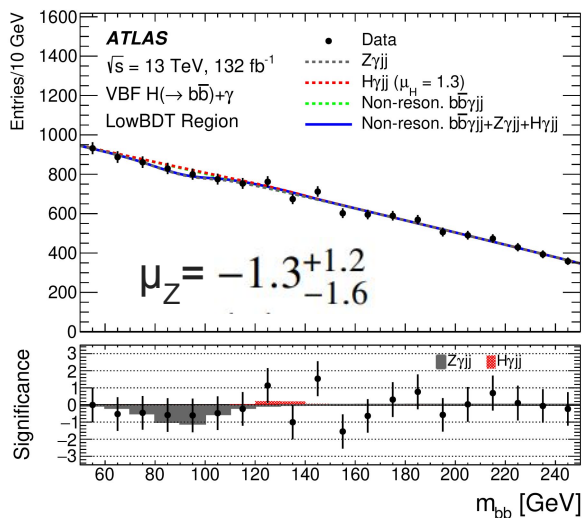


Signal+Background Fits

Signal+background fits in each region

Float both Z and H components' normalizations, uncorrelating Z yields between regions

Increasing score 



Uncertainties

Source of absolute uncertainty	$\sigma(\mu_H)$ down	$\sigma(\mu_H)$ up
Statistical		
Data statistical	-0.78	+0.80
Bkg. fit shapes	-0.19	+0.22
Bkg. fit normalizations	-0.51	+0.52
Z boson normalizations	-0.15	+0.14
Systematic		
Spurious signal	-0.24	+0.21
Theoretical	-0.01	+0.08
Photon	-0.01	+0.03
Jet	-0.06	+0.20
<i>b</i> -tagging	-0.02	+0.11
Auxiliary	-0.01	+0.04
Total	-0.99	+1.04
Total statistical	-0.96	+0.99
Total systematic	-0.25	+0.32

Statistical uncertainties dominant

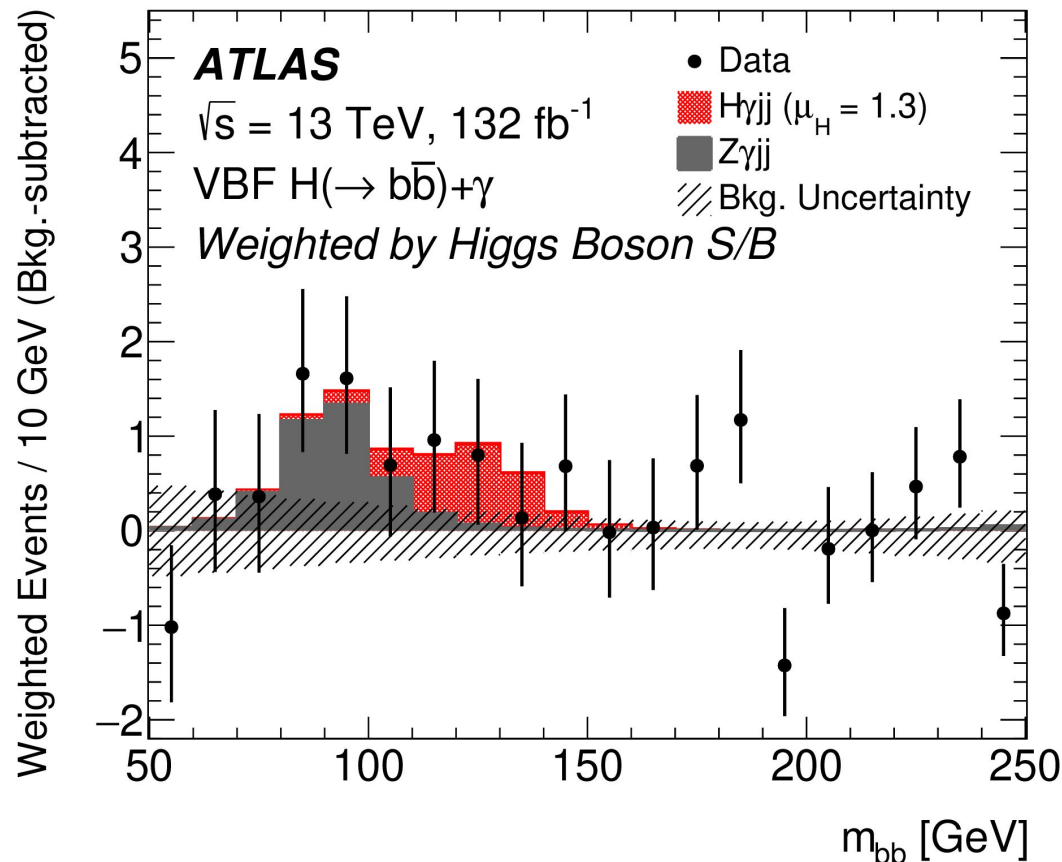
Systematics on multijet background

Signal uncertainties (theory + object)

Results

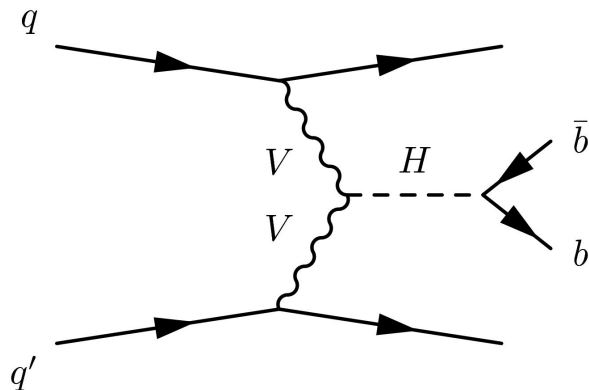
Observe (expect)

- 1.3σ (1.0σ)
- $\mu_{H \rightarrow bb} = 1.3 \pm 1.0$ (1.0 ± 1.0)
- $\mu_{\text{VBF } H \rightarrow bb} = 1.3 \pm 1.0$ (1.0 ± 1.0)



Fully Hadronic VBF $H \rightarrow b\bar{b}$

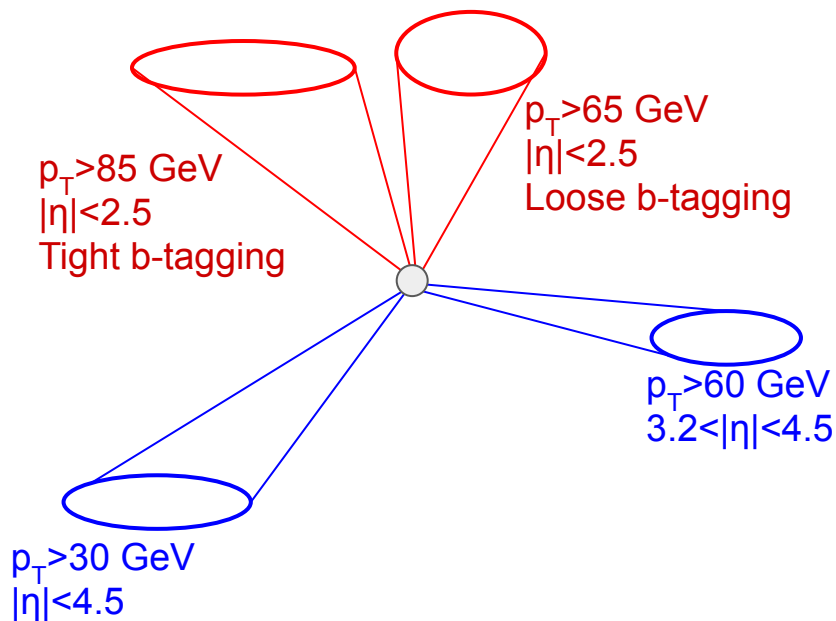
- Search for VBF $H \rightarrow b\bar{b}$ in a fully hadronic final state
- MVA approach to categorize events
- Fit signal and background on $m_{b\bar{b}}$ distribution
- **Analysis dramatically different from 2016 result, resulting in significant improvement to sensitivity (beyond improvement in statistics)**
- Expected 0.5σ with 2016 data -
extrapolating to Run 2 dataset, would expect 1.1σ



Analysis Channels and Selection

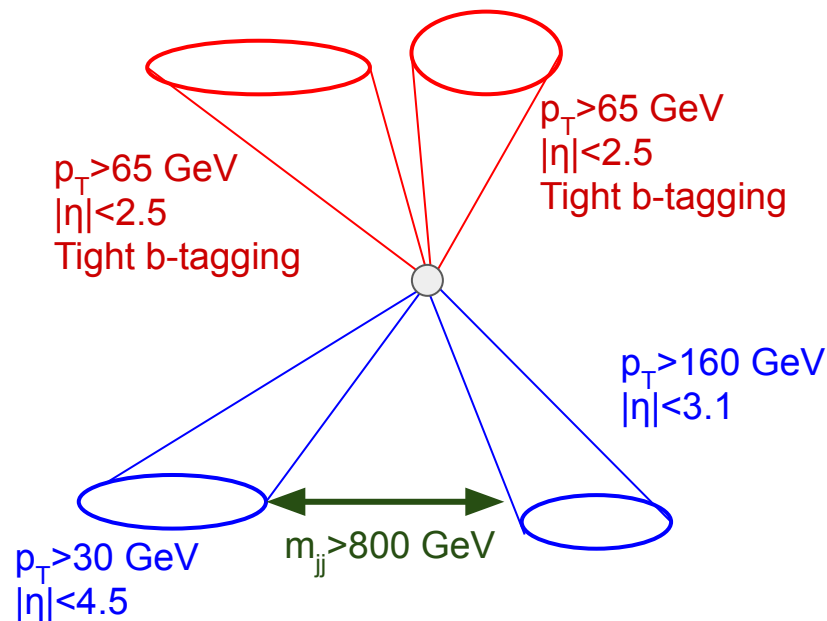
Forward Channel

Events contain a high p_T forward jet



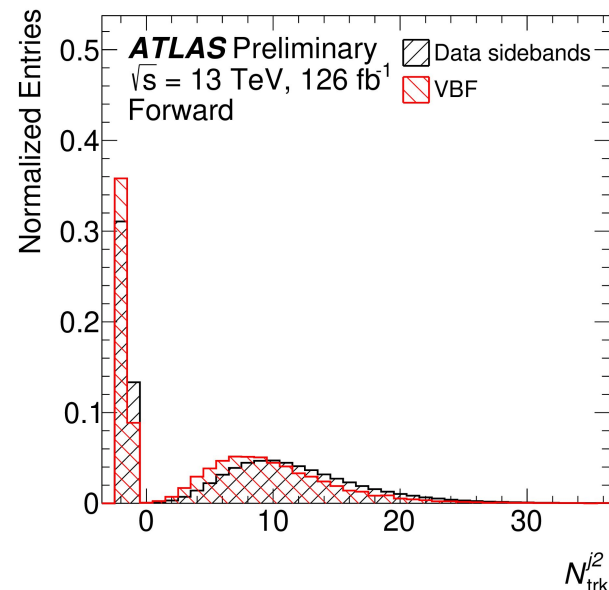
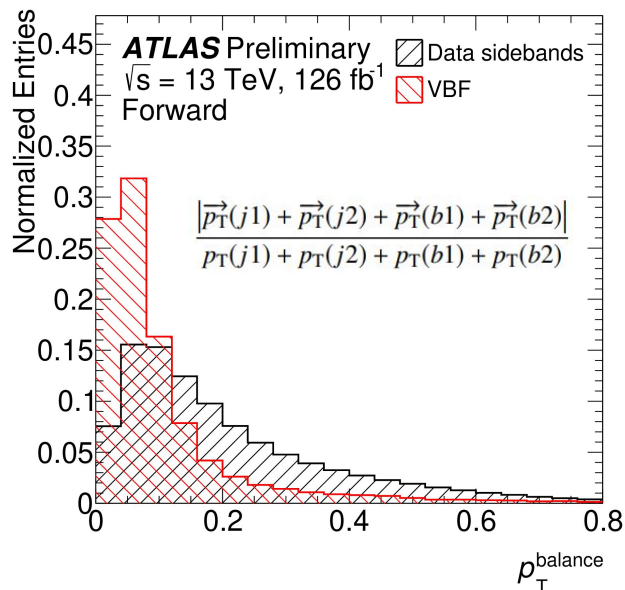
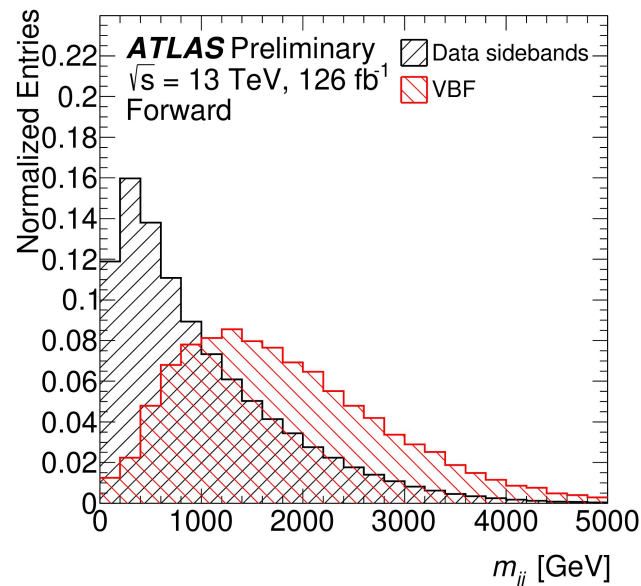
Central Channel

Events do not contain a high p_T forward jet



Signal/Background Discrimination

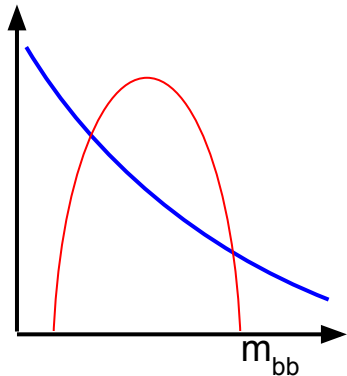
- MVA to categorize events, based on set of input kinematic variables
- Strongest discriminants based on angular separation of jets or on the presence of extra jets or soft emissions
- Extra discrimination comes from, for example, quark/gluon tagging



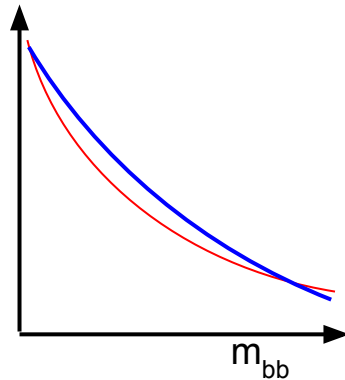
Adversarial Neural Network

- MVA variables chosen to be largely uncorrelated with m_{bb}
- Residual correlations still possible, particularly when combining variables in MVA
- Train an **adversarial neural network** in each channel, effectively adding a term to the loss function to explicitly penalize a network that correlates m_{bb} and score
- Training performed between signal and data sidebands

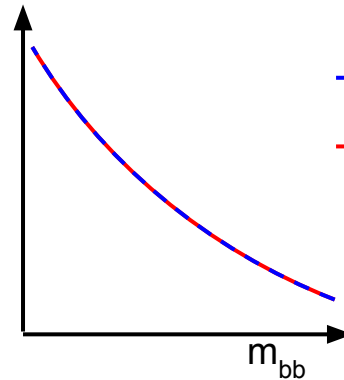
All variables



m_{bb} -independent variables



ANN with m_{bb} -independent variables

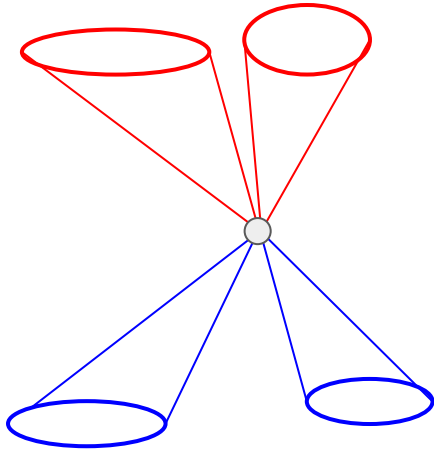


— Low score events
— High score events

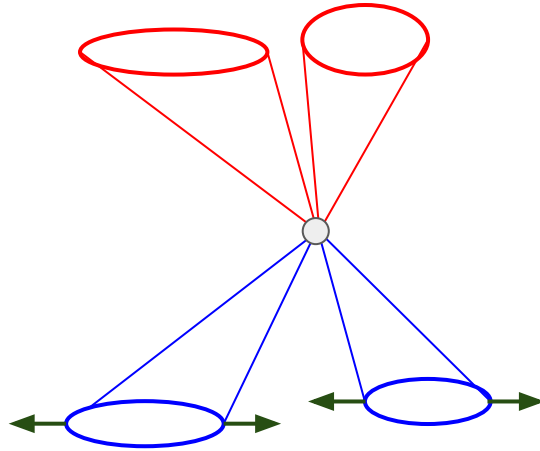
Background Uncertainties

Define CRs to measure any potential bias induced by excluding Higgs mass window

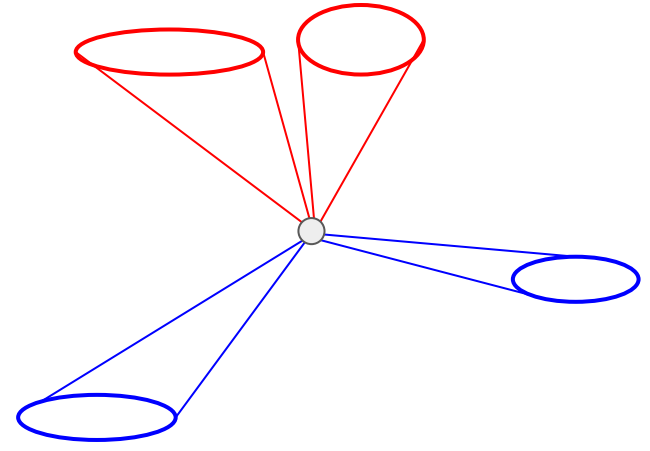
Select events with low m_{jj}
and no forward jets



Smear VBF jet η to
mimic SR kinematics



Reweight event-kinematics to
remove residual SR-CR differences



Fit signal+background to CRs to measure maximum possible bias

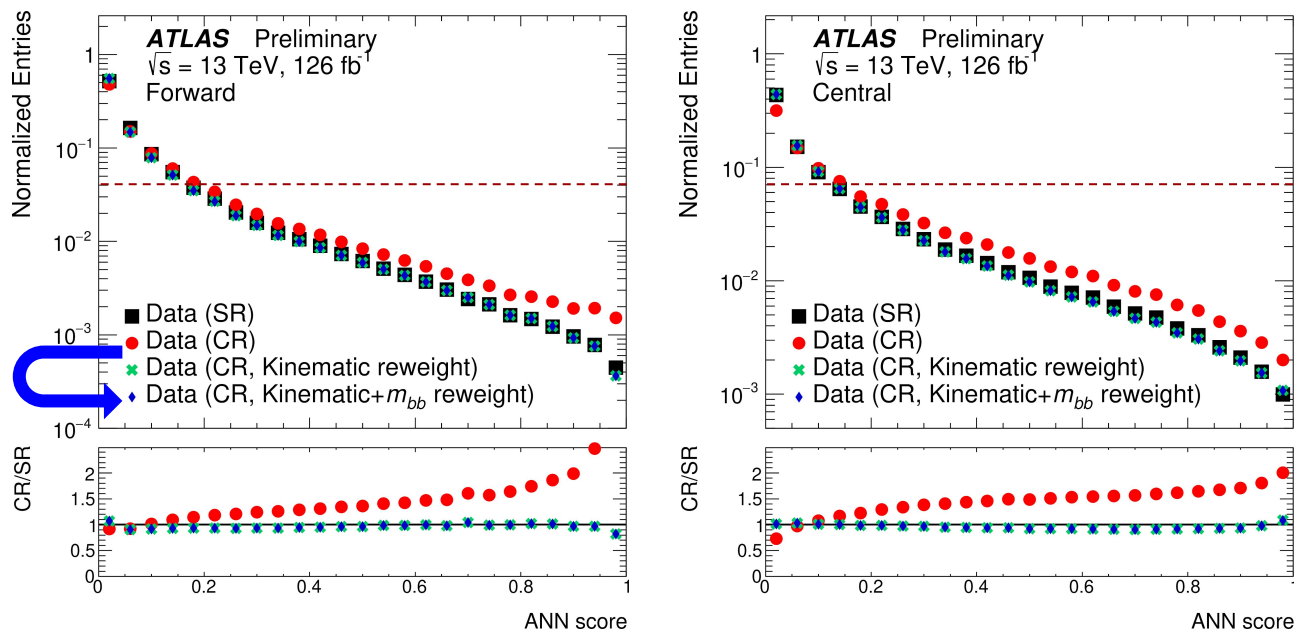
Classifier and CRs

Score distributions shown in SR, for each ANN

Score distribution shown for CR, **before** kinematic CR \rightarrow SR reweighting, **after** reweighting (except m_{bb}), and **after** reweighting m_{bb}

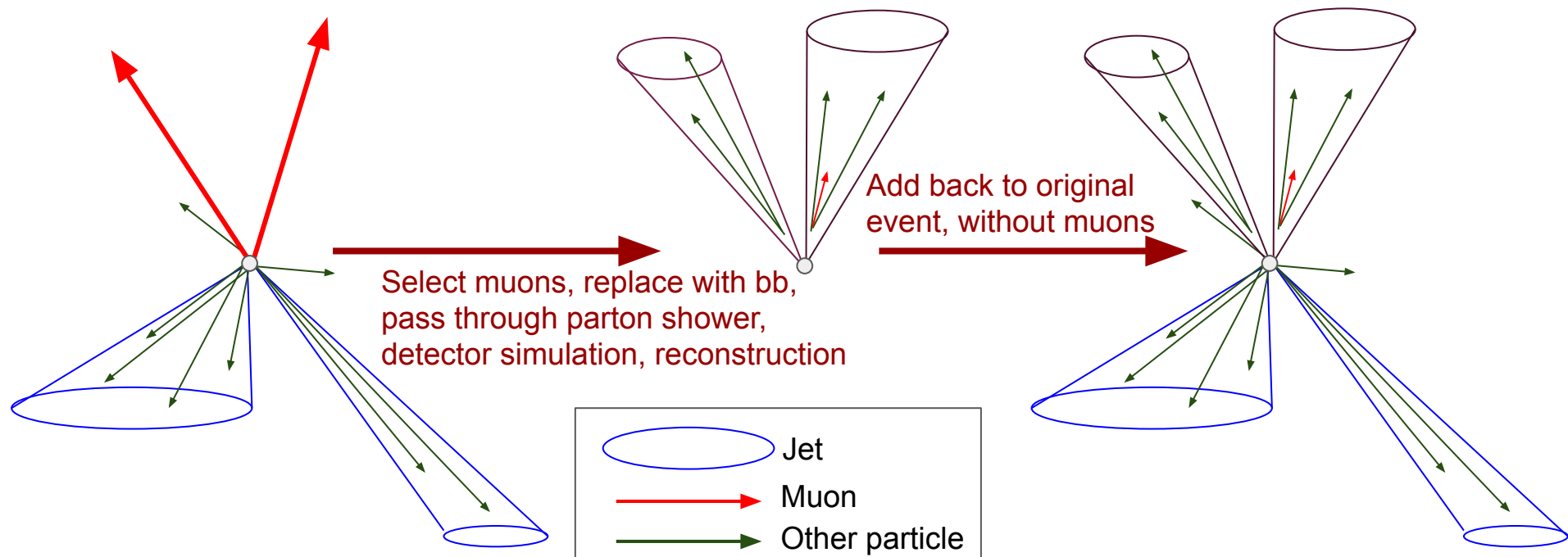
VBF distribution flat from 0 to 1 (at 0.04 in these figures)

Reweight variables in CR to match SR



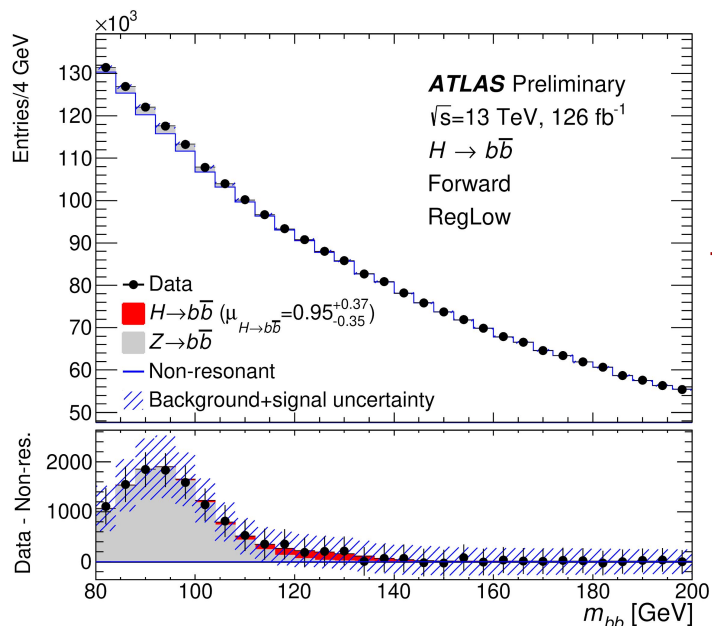
Z→bb Background

- Potentially significant mismodeling and systematic uncertainties
- Due to trigger limitations, cannot constrain Z in fits
→Data-driven approach: estimate Z→bb from Z→μμ (embedding)

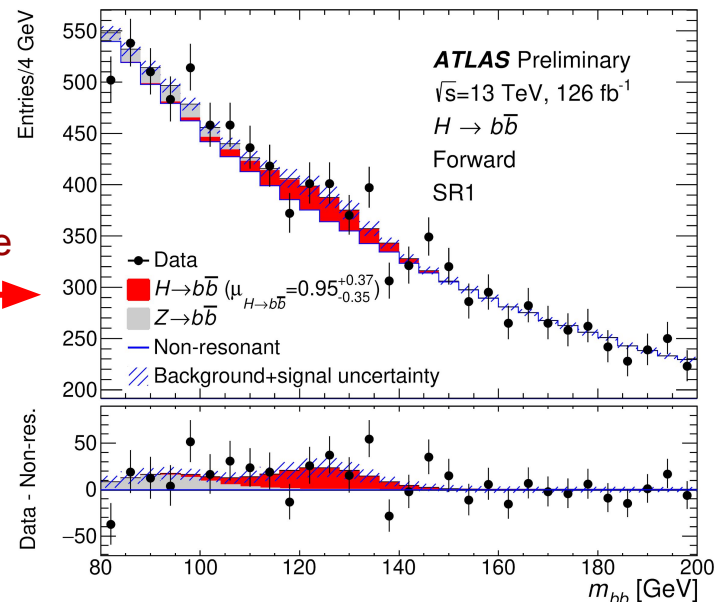


Fits (Forward Channel)

- Fit 4 high score regions + one low score region in each channel (10 regions total)
- Score and m_{bb} uncorrelated \rightarrow constrain background template in high score signal regions using high-statistic low score control region



Take background shape



Uncertainties

Uncertainty	$\sigma(\mu_{H \rightarrow bb})$
Statistical	± 0.31
Background shape	± 0.15
Resonant background	± 0.05
Theory	+0.06, -0.03
Object	+0.10, -0.05

Statistical uncertainties dominate

Uncertainties from CRs

Uncertainties from data-driven $Z \rightarrow bb$ estimate

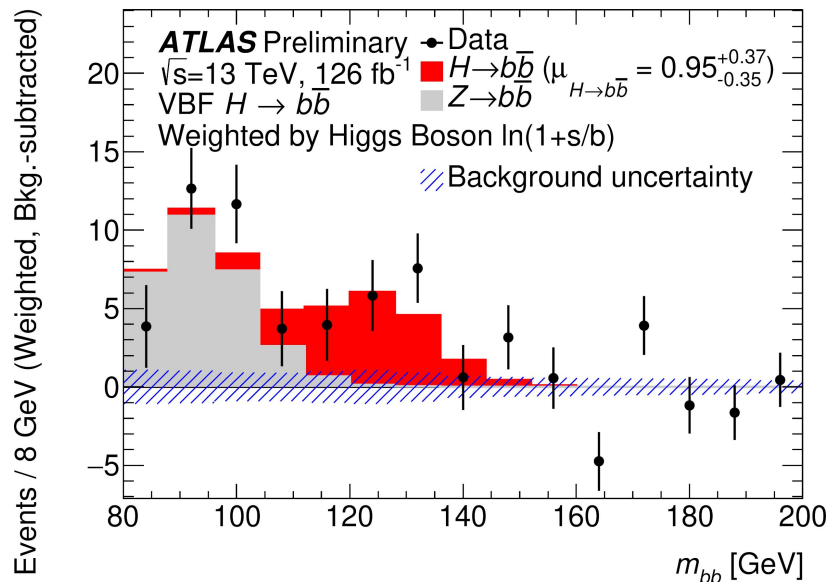
Theory uncertainties, signal only

Other uncertainties, signal only
(trigger, jet energy, b-tagging, etc.)

Results

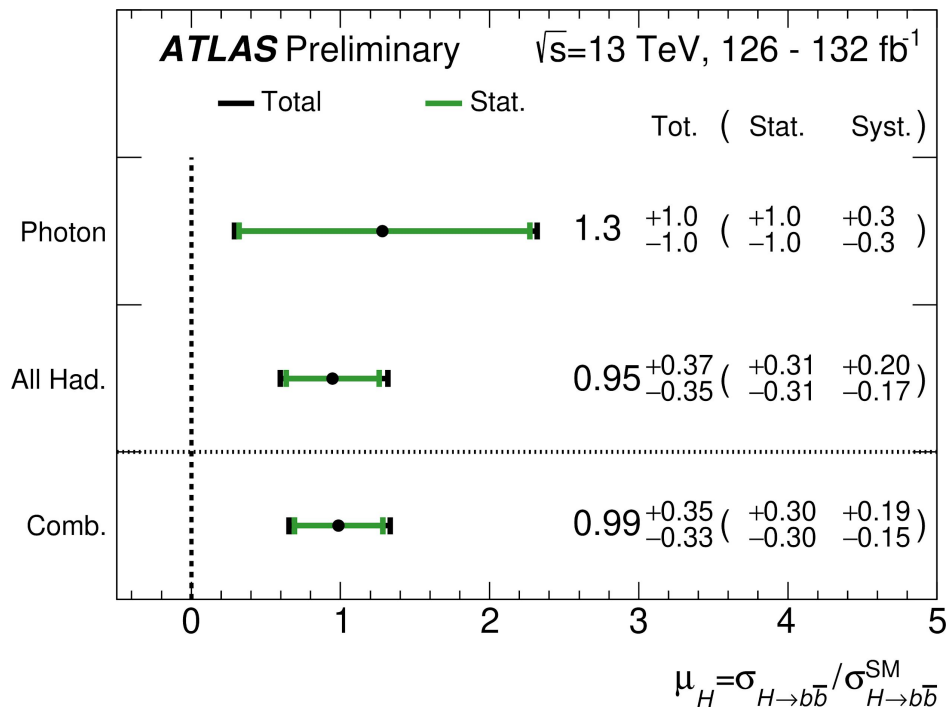
Observe (expect):

Inclusive $H \rightarrow bb$ production	2.7σ (2.9σ)	$\mu = 0.95^{+0.37}_{-0.35}$ ($1.00^{+0.37}_{-0.36}$)
VBF $H \rightarrow bb$ production	2.6σ (2.8σ)	$\mu = 0.95^{+0.38}_{-0.36}$ ($1.00^{+0.38}_{-0.37}$)
Inclusive $H \rightarrow bb$ production for $p_T^H > 200$ GeV	2.2σ (2.3σ)	$\mu = 0.93^{+0.45}_{-0.43}$ ($1.00^{+0.45}_{-0.43}$)



Combination

- Combination of all-hadronic VBF $H \rightarrow b\bar{b}$ and VBF $H + \gamma$ results
- Statistical uncertainties dominant
- Observe (expect) 3.0σ (3.0σ) for $H \rightarrow b\bar{b}$ production and 2.9σ (2.9σ) for VBF $H \rightarrow b\bar{b}$



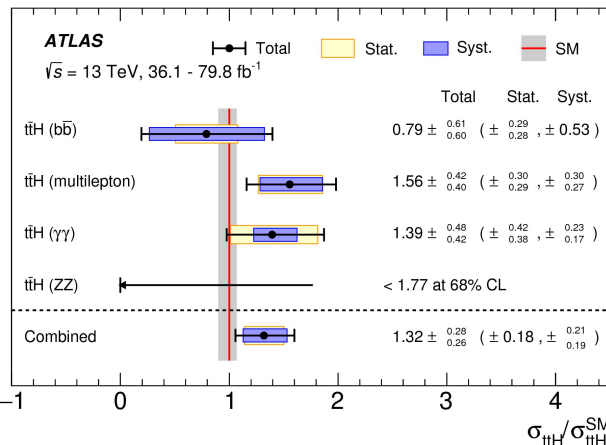
ttH: History

ttH is sensitive to many BSM effects, but precise measurement is difficult due to small cross-section (0.5 pb)

ttH observed by CMS and ATLAS with 2015-2016 or 2015-2017 data, combining ttH(bb), ttH($\gamma\gamma$), ttH(4l), and ttH(multilepton)

Updated measurements include full Run 2 dataset for ttH($\gamma\gamma$)

Low ttH($\gamma\gamma$) statistics at high $p_T^H \rightarrow$ make high p_T^H measurements with ttH(bb)



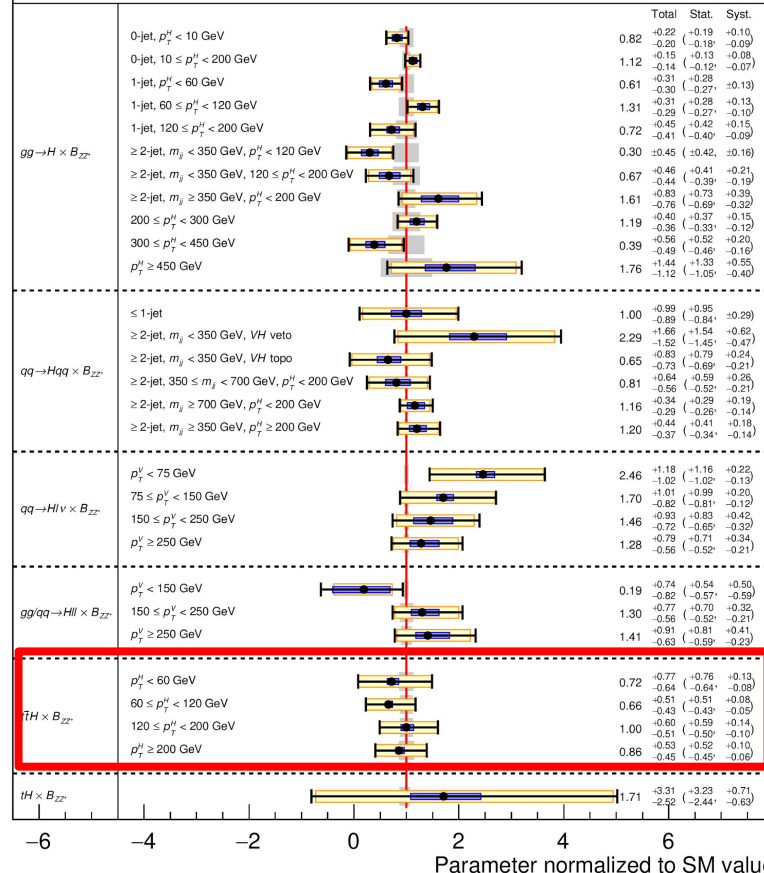
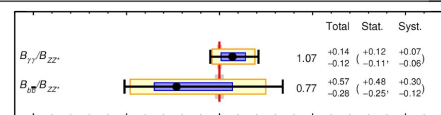
arXiv:1806.00425

ATLAS-CONF-2020-027

ATLAS Preliminary

$\sqrt{s} = 13 \text{ TeV}, 139 \text{ fb}^{-1}$
 $m_H = 125.09 \text{ GeV}, |\gamma_H| < 2.5$
 $p_{\text{SM}} = 95\%$

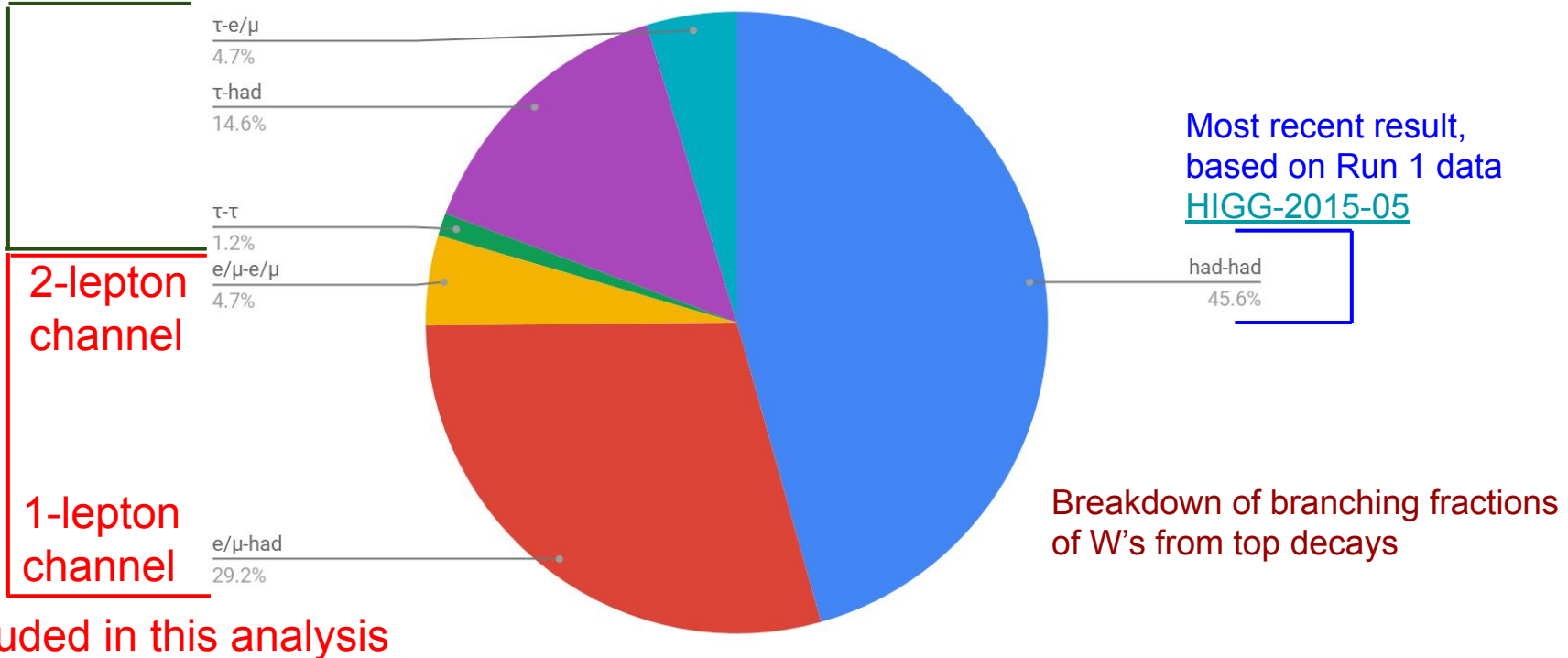
Legend: Total (black dot), Stat. (yellow bar), Syst. (blue bar), SM (grey bar)



$ttH \rightarrow bb$

Events categorized based on lepton multiplicity into 1-lepton and 2-lepton channels

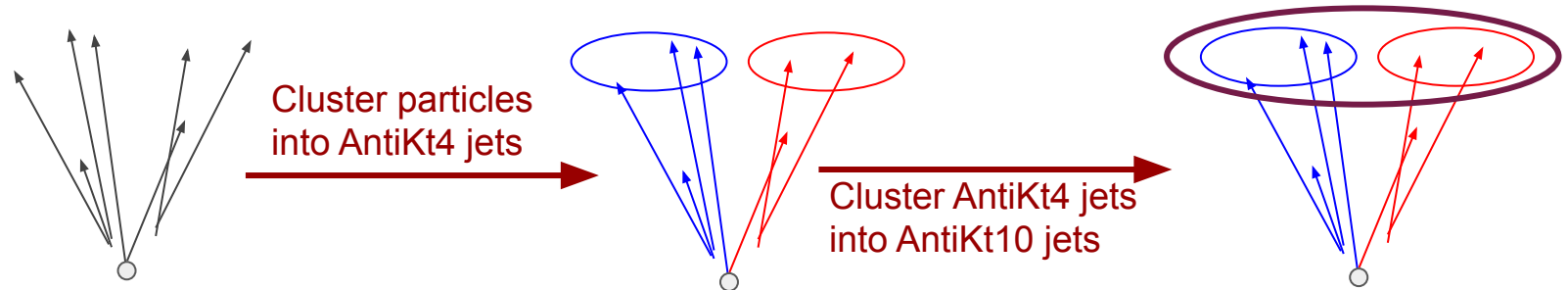
Hadronic τ decays not included, for orthogonality with other channels



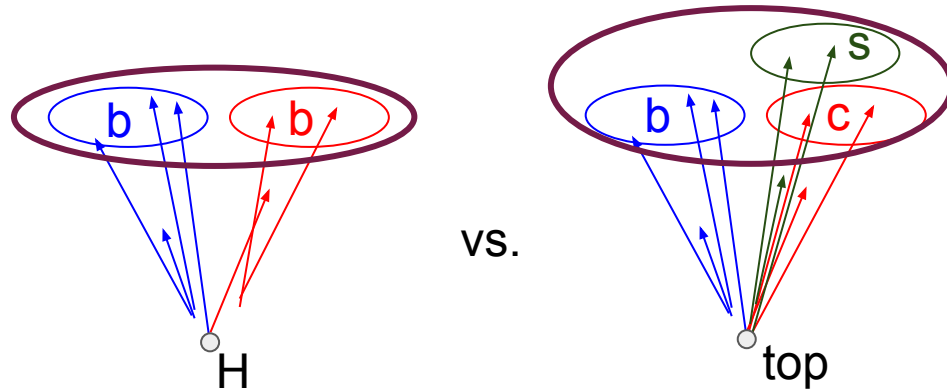
Boosted vs. Resolved Channels

$ttH \rightarrow bb$ 1-lepton channel split into boosted and resolved channels

Remove events from resolved channel that contain large-R jet passing selection



DNN to discriminate $H \rightarrow bb$ from tt or other backgrounds:



Largely relies on b-tagging and mass information

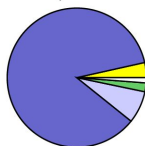
[ATLAS-CONF-2020-058](#)

Regions and Backgrounds

0-120 GeV | 120-200 GeV | 200-300 GeV | 300-(450 GeV) | 450- GeV

ATLAS Preliminary
 $\sqrt{s} = 13$ TeV
 Dilepton

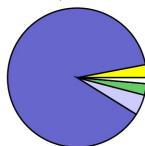
$SR_{\geq 4b}^{\geq 4j}, p_T^H \in [0, 120)$



2-lepton
 ≥ 4 b-jets
 ≥ 4 jets

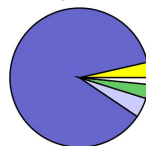
120-200 GeV

$SR_{\geq 4b}^{\geq 4j}, p_T^H \in [120, 200)$



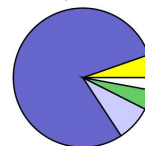
200-300 GeV

$SR_{\geq 4b}^{\geq 4j}, p_T^H \in [200, 300)$



300-(450 GeV)

$SR_{\geq 4b}^{\geq 4j}, p_T^H \in [300, \infty)$



450- GeV

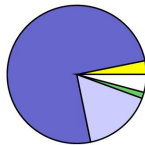
Split into pTH bins,
 matching STXS pTH bins

tt+≥1b is main
 background in all regions

Legend:
 □ $tt + li., 4t, tH$ ■ $tt + V$
 □ $tt + \geq 1c$ ■ $tt + \geq 1b$
 ■ Other

ATLAS Preliminary
 $\sqrt{s} = 13$ TeV
 Single lepton

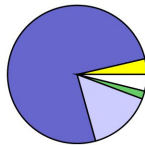
$SR_{\geq 4b}^{\geq 6j}, p_T^H \in [0, 120)$



1-lepton
 (resolved)
 ≥ 4 b-jets
 ≥ 6 jets

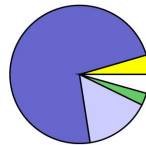
120-200 GeV

$SR_{\geq 4b}^{\geq 6j}, p_T^H \in [120, 200)$



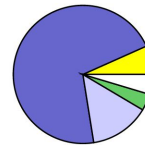
200-300 GeV

$SR_{\geq 4b}^{\geq 6j}, p_T^H \in [200, 300)$



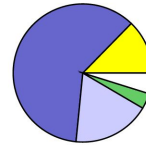
300-(450 GeV)

$SR_{\geq 4b}^{\geq 6j}, p_T^H \in [300, 450)$



450- GeV

$SR_{\geq 4b}^{\geq 6j}, p_T^H \in [450, \infty)$

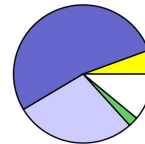


Legend:
 □ $tt + li., 4t, tH$ ■ $tt + V$
 □ $tt + \geq 1c$ ■ $tt + \geq 1b$
 ■ Other

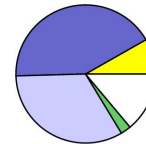
1-lepton (boosted)

≥ 2 b-jets
 ≥ 4 jets
 \geq boosted cand.

$SR_{\text{boosted}}^{\geq 4j}, p_T^H \in [300, 450)$

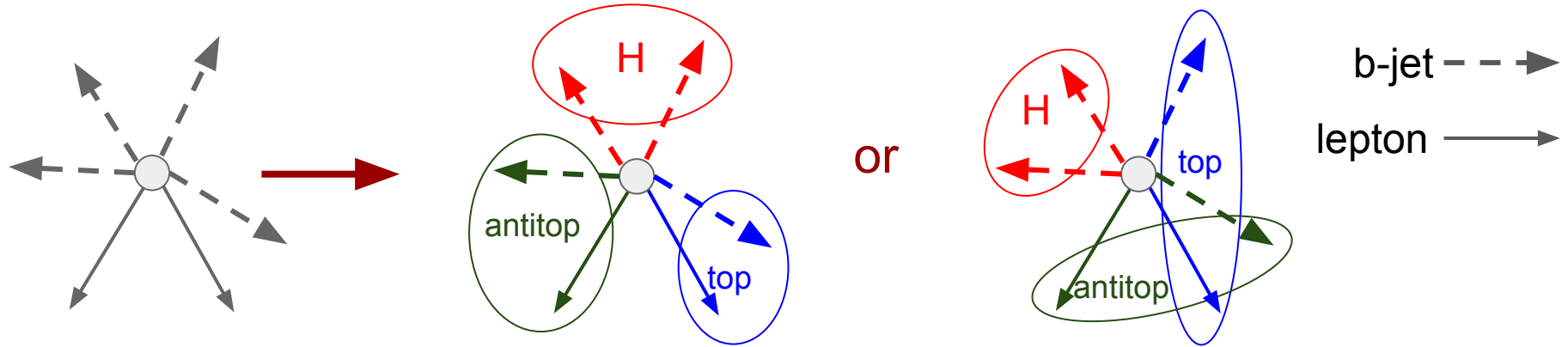


$SR_{\text{boosted}}^{\geq 4j}, p_T^H \in [450, \infty)$



BDTs

Reconstruction BDTs: In non-boosted channels, group jets, leptons, and E_T^{miss} into H, W, top, and antitop candidates to calculate input variables and p_T^{bb}



Classification BDTs: discriminate signal from background, using as input kinematic properties of input objects, as well as reconstruction BDTs

Classification BDTs used in signal+background fits in signal regions

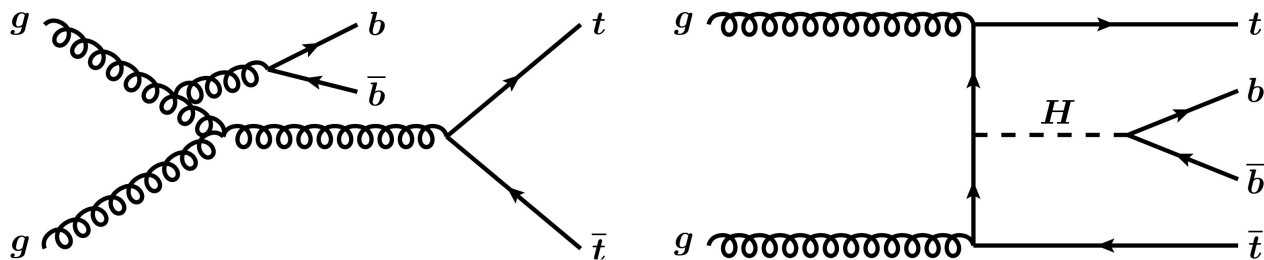
Background Estimate Overview

tt+light jets is small, due to tightened and simplified b-jet requirements
→ little overall impact from modeling uncertainties

tt+≥1b largest background in all regions

New: ttbb Powheg+Pythia8 4FS used in analysis as nominal tt+≥1b estimate

Define CRs to constrain **tt+≥1b** and **tt+≥1c**



Rely on presence of fewer b-tagged jets in **tt+≥1c** and lower jet multiplicity (above p_T thresholds) in tt+jets than ttH

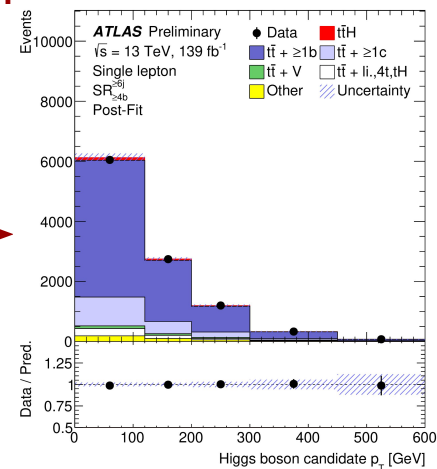
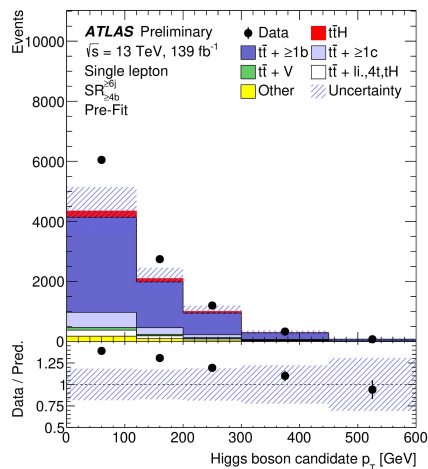
Background Modeling

- Extra parameters to account for potential mis-modeling in analysis phase space
- Dominant background normalization $k(tt+\geq 1b)$ is floated in fit (but not $tt+\geq 1c$)
- Other notable changes compared to 2016 analysis
 - 2-point systematic 4FS-vs-5FS removed from the analysis model
 - Effective statistics of alternative simulated samples dramatically increased

Uncertainty source	Description	Components
$t\bar{t}$ cross-section	$\pm 6\%$	$t\bar{t}$ + light
$t\bar{t} + \geq 1b$ normalisation	Free-floating	$t\bar{t} + \geq 1b$
$t\bar{t} + \geq 1c$ normalisation	$\pm 100\%$	$t\bar{t} + \geq 1c$
NLO matching	MADGRAPH5_aMC@NLO+PYTHIA8 vs. POWHEGBOX+PYTHIA8	All
PS & hadronisation	POWHEGBOX+HERWIG7 vs. POWHEGBOX+PYTHIA8	All
ISR	Varying α_S^{ISR} (PS), μ_R & μ_F (ME)	in POWHEGBOXRES+PYTHIA8 $t\bar{t} + \geq 1b$ in POWHEGBOX+PYTHIA8 $t\bar{t} + \geq 1c, t\bar{t}$ + light
FSR	Varying α_S^{FSR} (PS)	in POWHEGBOXRES+PYTHIA8 $t\bar{t} + \geq 1b$ in POWHEGBOX+PYTHIA8 $t\bar{t} + \geq 1c, t\bar{t}$ + light
$t\bar{t} + \geq 1b$ fractions	POWHEGBOX+HERWIG7 vs. POWHEGBOX+PYTHIA8	$t\bar{t} + 1b/1B, t\bar{t} + \geq 2b$
p_T^{bb} shape	Shape mismodelling measured from data	$t\bar{t} + \geq 1b$

Background Modeling: p_T^{bb}

Shape parameter introduced to account for potential shape differences between data and MC



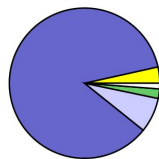
Uncertainty source	Description	Components	
$t\bar{t}$ cross-section	$\pm 6\%$	$t\bar{t}$ + light	
$t\bar{t} + \geq 1b$ normalisation	Free-floating	$t\bar{t} + \geq 1b$	
$t\bar{t} + \geq 1c$ normalisation	$\pm 100\%$	$t\bar{t} + \geq 1c$	
NLO matching	MADGRAPH5_aMC@NLO+PYTHIA8 vs. POWHEGBOX+PYTHIA8	All	
PS & hadronisation	POWHEGBOX+HERWIG7 vs. POWHEGBOX+PYTHIA8	All	
ISR	Varying α_S^{ISR} (PS), μ_R & μ_F (ME)	in POWHEGBOXRES+PYTHIA8	$t\bar{t} + \geq 1b$
		in POWHEGBOX+PYTHIA8	$t\bar{t} + \geq 1c$, $t\bar{t}$ + light
FSR	Varying α_S^{FSR} (PS)	in POWHEGBOXRES+PYTHIA8	$t\bar{t} + \geq 1b$
		in POWHEGBOX+PYTHIA8	$t\bar{t} + \geq 1c$, $t\bar{t}$ + light
$t\bar{t} + \geq 1b$ fractions	POWHEGBOX+HERWIG7 vs. POWHEGBOX+PYTHIA8	$t\bar{t} + 1b/1B$, $t\bar{t} + \geq 2b$	
p_T^{bb} shape	Shape mismodelling measured from data	$t\bar{t} + \geq 1b$	

Background Modeling: Dilepton

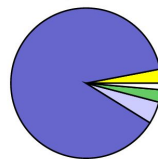
ATLAS Preliminary
 $\sqrt{s} = 13$ TeV
 Dilepton

\square $t\bar{t} + li, 4t, tH$ \blacksquare $t\bar{t} + V$
 \square $t\bar{t} + \geq 1c$ \blacksquare $t\bar{t} + \geq 1b$
 \blacksquare Other

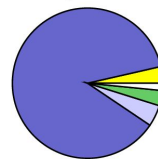
$SR_{\geq 4b}^{\geq 4j}, p_T^H \in [0, 120]$



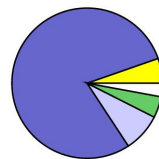
$SR_{\geq 4b}^{\geq 4j}, p_T^H \in [120, 200]$



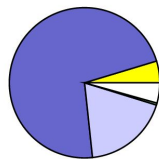
$SR_{\geq 4b}^{\geq 4j}, p_T^H \in [200, 300]$



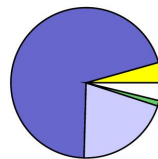
$SR_{\geq 4b}^{\geq 4j}, p_T^H \in [300, \infty)$



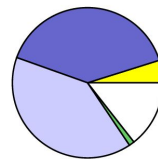
$CR_{3b\ hi}^{3j}$



$CR_{3b\ hi}^{\geq 4j}$



$CR_{3b\ lo}^{\geq 4j}$



Dilepton CRs with loosened b-tagging and also including 3j events

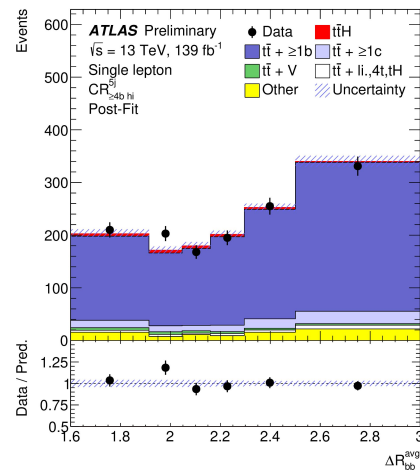
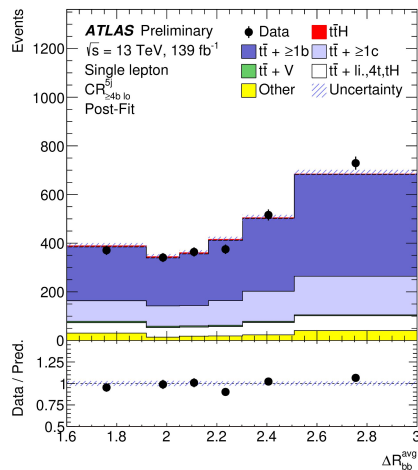
Constrain relative normalization of each $t\bar{t}$ background

Uncertainty source	Description	Components
$t\bar{t}$ cross-section	$\pm 6\%$	$t\bar{t} + \text{light}$
$t\bar{t} + \geq 1b$ normalisation	Free-floating	$t\bar{t} + \geq 1b$
$t\bar{t} + \geq 1c$ normalisation	$\pm 100\%$	$t\bar{t} + \geq 1c$
NLO matching	MADGRAPH5_aMC@NLO+PYTHIA8 vs. POWHEGBOX+PYTHIA8	All
PS & hadronisation	POWHEGBOX+HERWIG7 vs. POWHEGBOX+PYTHIA8	All
ISR	Varying α_S^{ISR} (PS), μ_R & μ_F (ME)	in POWHEGBOXRES+PYTHIA8: $t\bar{t} + \geq 1b$ in POWHEGBOX+PYTHIA8: $t\bar{t} + \geq 1c, t\bar{t} + \text{light}$
FSR	Varying α_S^{FSR} (PS)	in POWHEGBOXRES+PYTHIA8: $t\bar{t} + \geq 1b$ in POWHEGBOX+PYTHIA8: $t\bar{t} + \geq 1c, t\bar{t} + \text{light}$
$t\bar{t} + \geq 1b$ fractions	POWHEGBOX+HERWIG7 vs. POWHEGBOX+PYTHIA8	$t\bar{t} + 1b/1B, t\bar{t} + \geq 2b$
p_T^{bb} shape	Shape mismodelling measured from data	$t\bar{t} + \geq 1b$

Background Modeling: Single Lepton

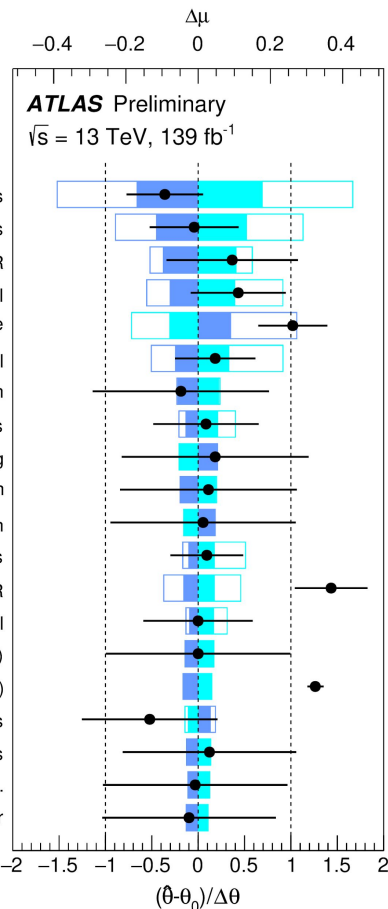
Single lepton CRs with low n-jets

Constrain kinematic variable shape and constrain relative normalization of each $t\bar{t}$ background



Uncertainty source	Description	Components
$t\bar{t}$ cross-section	$\pm 6\%$	$t\bar{t}$ + light
$t\bar{t} + \geq 1b$ normalisation	Free-floating	$t\bar{t} + \geq 1b$
$t\bar{t} + \geq 1c$ normalisation	$\pm 100\%$	$t\bar{t} + \geq 1c$
NLO matching	MADGRAPH5_aMC@NLO+PYTHIA8 vs. POWHEGBOX+PYTHIA8	All
PS & hadronisation	POWHEGBOX+HERWIG7 vs. POWHEGBOX+PYTHIA8	All
ISR	Varying α_S^{ISR} (PS), μ_R & μ_F (ME)	in POWHEGBOXRES+PYTHIA8: $t\bar{t} + \geq 1b$ in POWHEGBOX+PYTHIA8: $t\bar{t} + \geq 1c, t\bar{t}$ + light
FSR	Varying α_S^{FSR} (PS)	in POWHEGBOXRES+PYTHIA8: $t\bar{t} + \geq 1b$ in POWHEGBOX+PYTHIA8: $t\bar{t} + \geq 1c, t\bar{t}$ + light
$t\bar{t} + \geq 1b$ fractions	POWHEGBOX+HERWIG7 vs. POWHEGBOX+PYTHIA8	$t\bar{t} + 1b/1B, t\bar{t} + \geq 2b$
p_T^{bb} shape	Shape mismodelling measured from data	$t\bar{t} + \geq 1b$

Uncertainty Breakdown

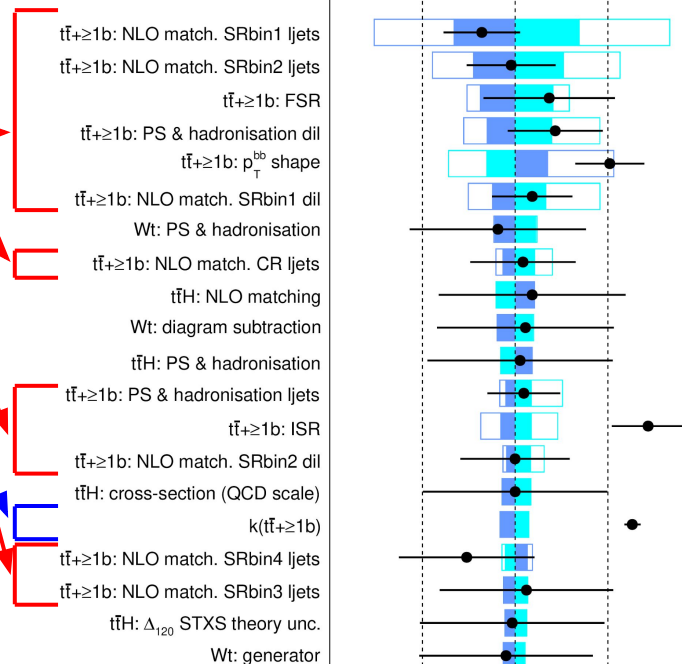
Pre-fit impact on μ :
 $\square \theta = \hat{\theta} + \Delta\theta$
 $\square \theta = \hat{\theta} - \Delta\theta$
Post-fit impact on μ :
 $\blacksquare \theta = \hat{\theta} + \Delta\hat{\theta}$
 $\blacksquare \theta = \hat{\theta} - \Delta\hat{\theta}$
 \bullet Nuis. Param. Pull


Uncertainty source	$\Delta\mu$	
$t\bar{t} + \geq 1b$ modelling	+0.25	-0.24
Total systematic uncertainty	+0.30	-0.27
$t\bar{t} + \geq 1b$ normalisation	+0.03	-0.05
Total statistical uncertainty	+0.20	-0.19
Total uncertainty	+0.36	-0.33

Dominant uncertainties relate to $t\bar{t} + \geq 1b$ modeling

$k(t\bar{t} + \geq 1b)$ has deviation from the expectation ($1.25^{+0.09}_{-0.08}$)

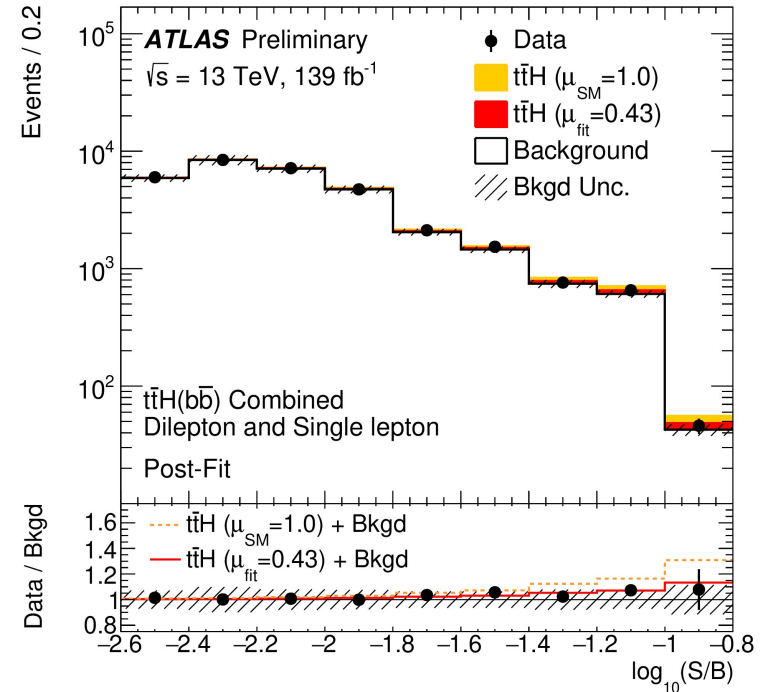
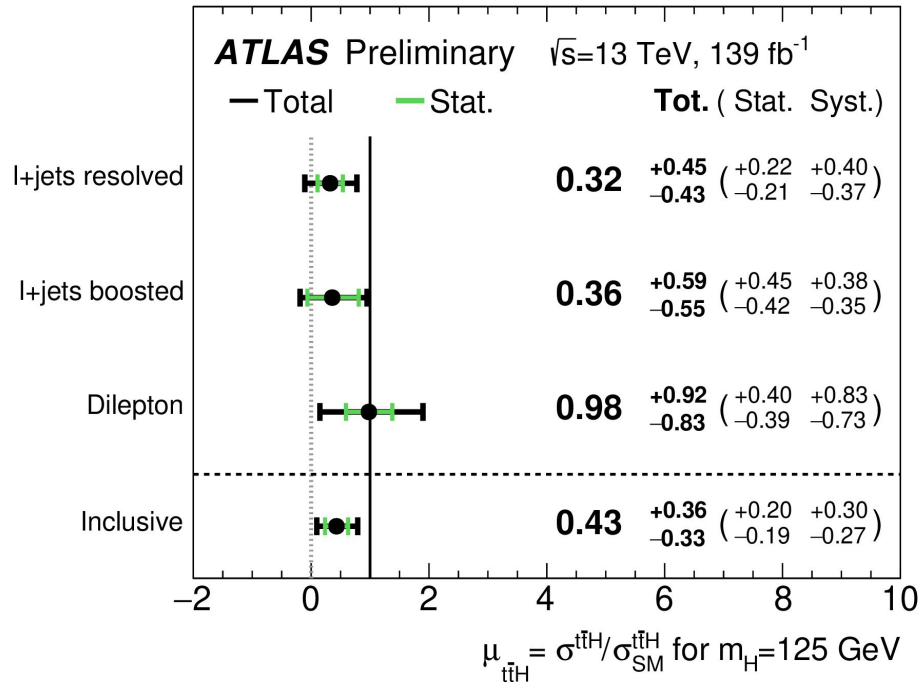
Better understanding of $t\bar{t} + \geq 1b$ processes will be key to further improvements of this measurement



Total Signal Strength

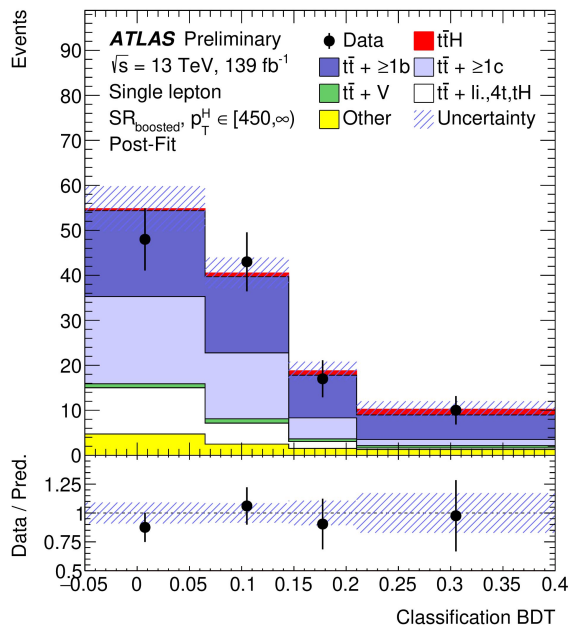
Inclusive measurement of $t\bar{t}H$ signal-strength:

$$\mu = 0.43^{+0.20}_{-0.19} \text{ (stat.) } ^{+0.30}_{-0.27} \text{ (syst.)} = 0.43^{+0.36}_{-0.33}$$

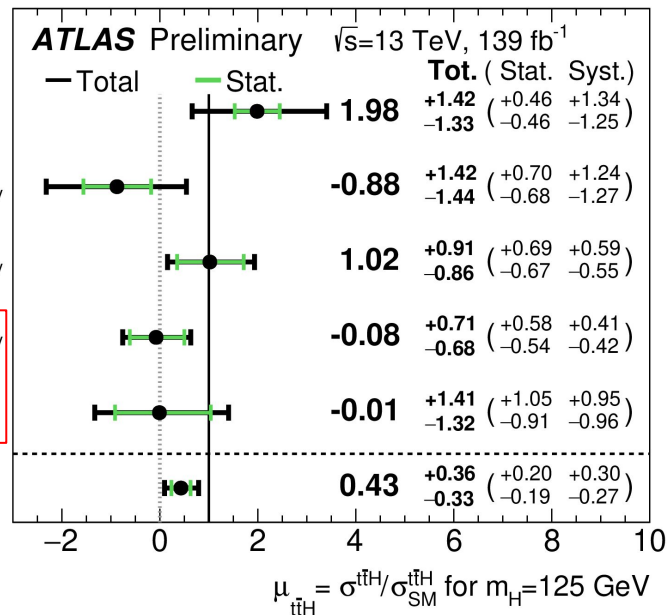


Results for p_T^H Measurement

Highest $t\bar{t}H$ p_T^H constraint ever with ATLAS!


 $\mu_{t\bar{t}H, p_T^H \in [0, 120] \text{ GeV}}$
 $\mu_{t\bar{t}H, p_T^H \in [120, 200] \text{ GeV}}$
 $\mu_{t\bar{t}H, p_T^H \in [200, 300] \text{ GeV}}$
 $\mu_{t\bar{t}H, p_T^H \in [300, 450] \text{ GeV}}$
 $\mu_{t\bar{t}H, p_T^H \in [450, \infty) \text{ GeV}}$

Inclusive



H → Invisible: History

Run 1

VBF, Z(lep)H, V(had)H

$$\mathcal{B}_{H \rightarrow \text{inv}} < 0.25 \quad (0.27^{+0.10}_{-0.08})$$

Run 1 + 2015-2016

VBF, Z(lep)H, V(had)H

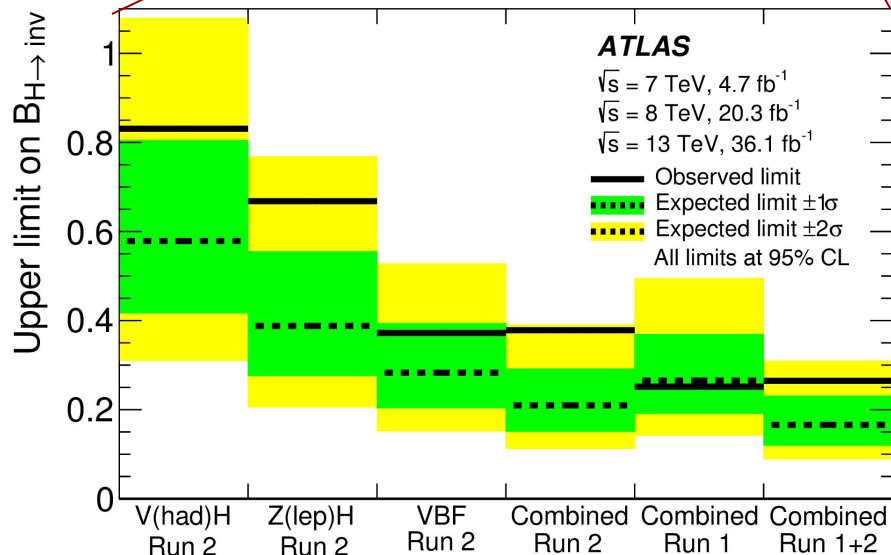
$$\mathcal{B}_{H \rightarrow \text{inv}} < 0.26 \quad (0.17^{+0.07}_{-0.05})$$

Run 1 + Run 2

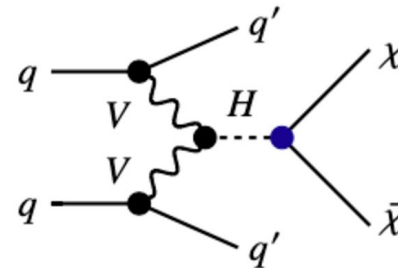
Run 1: VBF, Z(lep)H, V(had)H

Run 2: VBF, ttH

New result



VBF $H \rightarrow$ Invisible

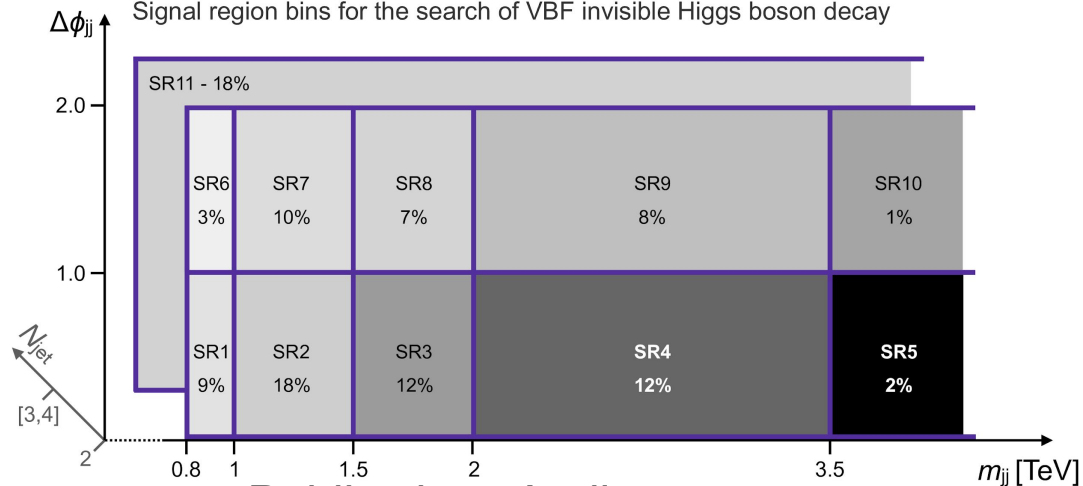


Require high E_T^{miss} , with VBF-like topology

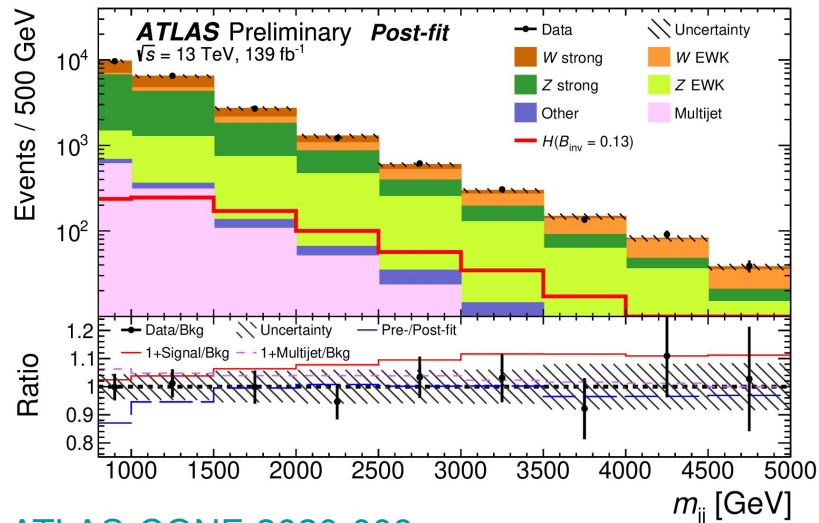
Divide events into SRs based on m_{jj} and $\Delta\phi$, with CRs to constrain normalization

ATLAS Preliminary, 139 fb⁻¹

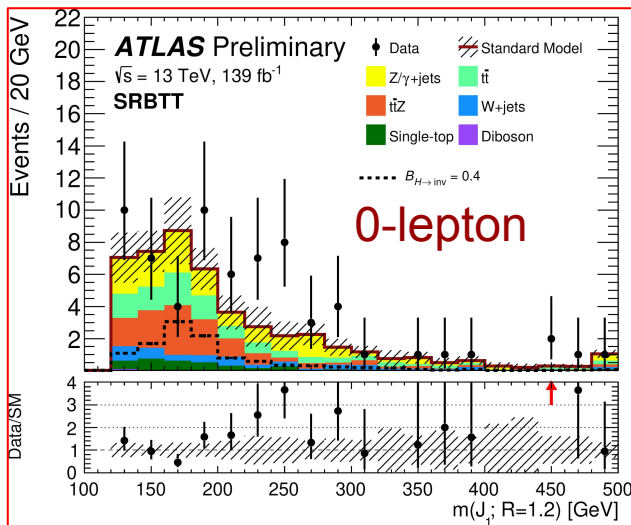
Signal region bins for the search of VBF invisible Higgs boson decay



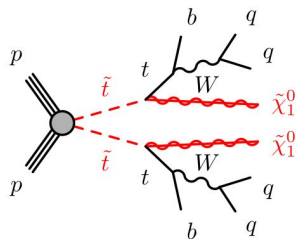
Public since April, discussed in [seminar](#)



[ATLAS-CONF-2020-008](#)



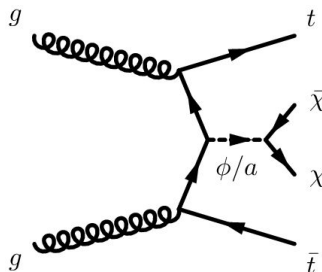
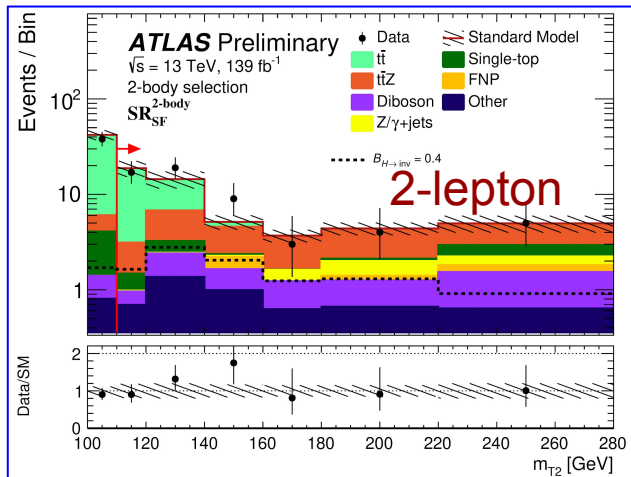
$t\bar{t}H \rightarrow \text{Invisible}$



Originally designed for high mass stop squarks

2 b-jets, $E_T^{\text{miss}} > 250 \text{ GeV}$, recluster jets into large-R jets representing top quarks

Reinterpretation of existing SUSY analyses, which targeted for example models given by these diagrams

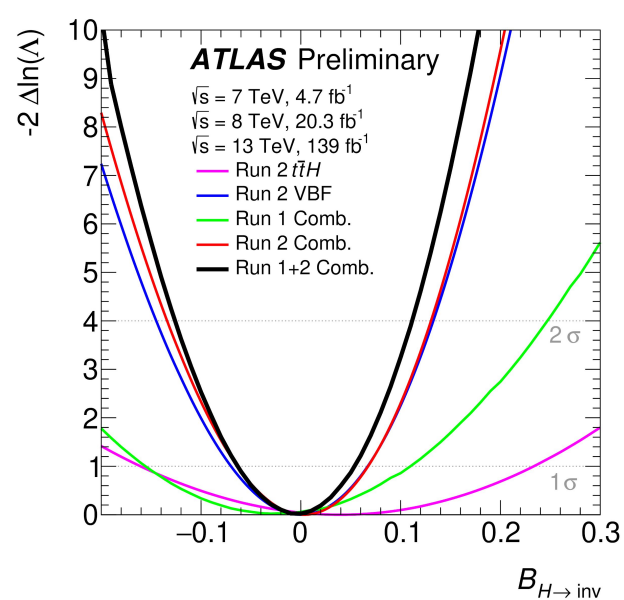


Selection designed for dark matter models

Requires ≥ 1 b-jet, with requirements placed on $E_T^{\text{miss, significance}}$ and m_{T2}

2L: [ATLAS-CONF-2020-046](#)

0L: [arXiv:2004.14060](#)



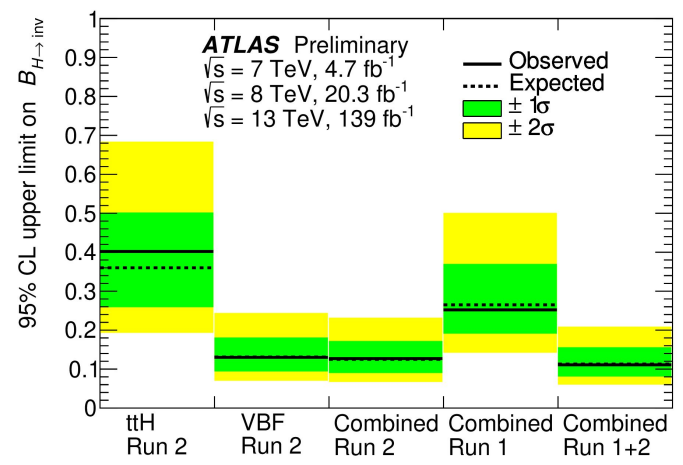
Combined $H \rightarrow \text{Invisible}$

95% CL

Analysis	\sqrt{s} [TeV]	Int. luminosity [fb $^{-1}$]	Best fit $\mathcal{B}_{H \rightarrow \text{inv}}$	Observed upper limit	Expected upper limit
Run 2 VBF	13	139	$0.00^{+0.07}_{-0.07}$	0.13	$0.13^{+0.05}_{-0.04}$
Run 2 $t\bar{t}H$	13	139	$0.04^{+0.20}_{-0.20}$	0.40	$0.36^{+0.15}_{-0.10}$
Run 2 Comb.	13	139	$0.00^{+0.06}_{-0.07}$	0.13	$0.12^{+0.05}_{-0.04}$
Run 1 Comb.	7, 8	4.7, 20.3	$-0.02^{+0.14}_{-0.13}$	0.25	$0.27^{+0.10}_{-0.08}$
Run 1+2 Comb.	7, 8, 13	4.7, 20.3, 139	$0.00^{+0.06}_{-0.06}$	0.11	$0.11^{+0.04}_{-0.03}$

Limit largely driven by VBF channel, with extra sensitivity contributed by $t\bar{t}H$ and full set of Run 1 measurements

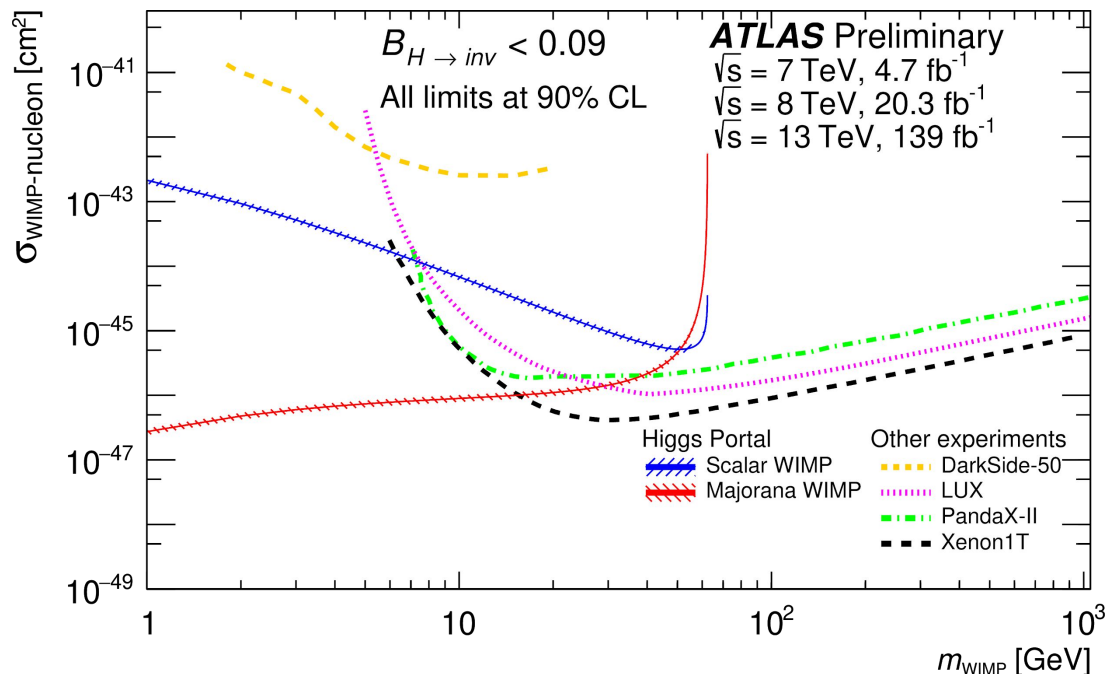
[ATLAS-CONF-2020-052](#)



H → Invisible in Context

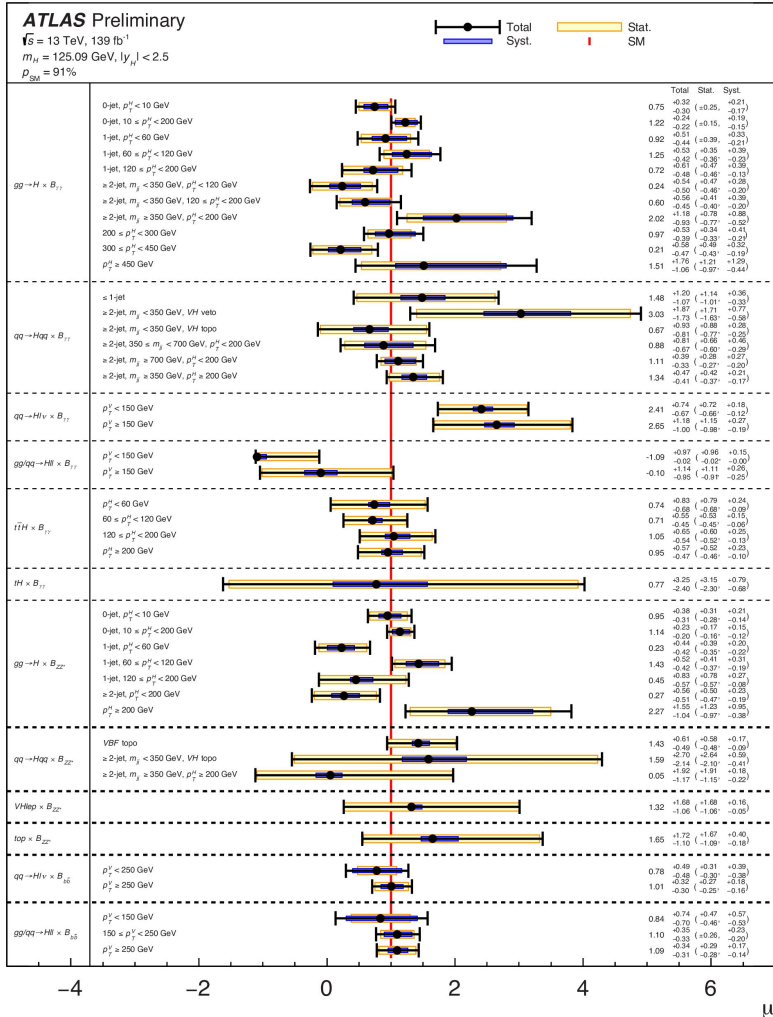
Comparison to direct detection experiments

The Higgs is assumed to decay to a pair of dark matter particles, either **scalars** or **Majorana fermions**



Higgs Properties: History

- Summer 2020 combination produced precise set of Higgs property measurements
- Result included coupling measurements and 2HDM interpretation
- Extended interpretation to MSSM and SMEFT



MSSM Interpretation

Interpretations for multiple different MSSM scenarios

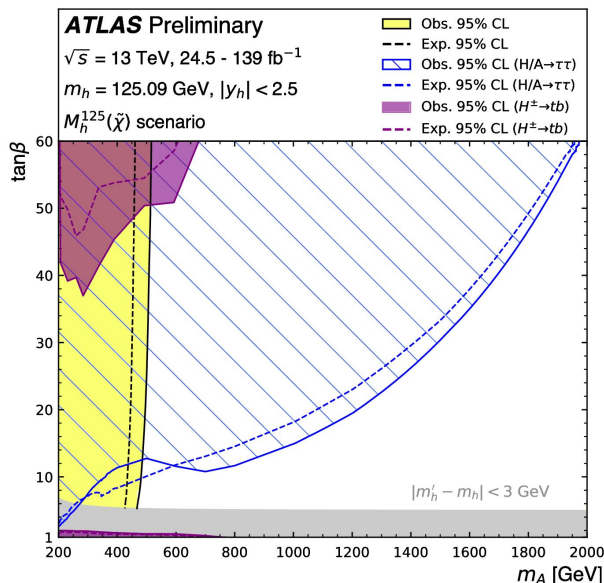
Examples given below, with comparison to direct searches

Includes cross-section measurements in all channels given in the table

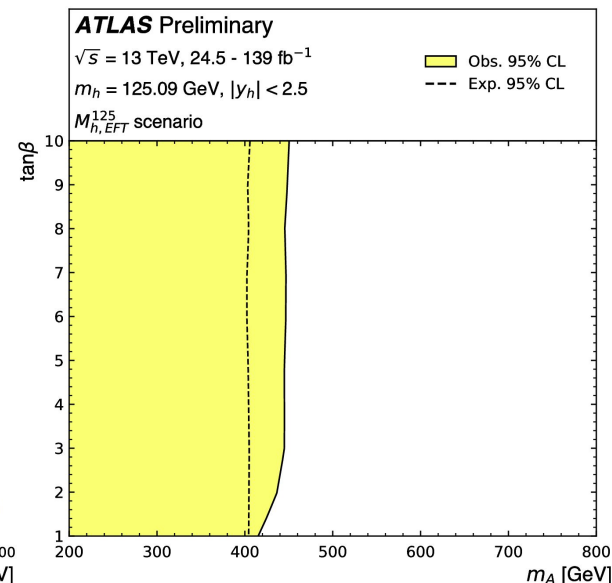
Analysis

$H \rightarrow \gamma\gamma$	(all production modes)
$H \rightarrow ZZ^* \rightarrow 4\ell$	(all production modes)
$H \rightarrow b\bar{b}$	(VH)
$H \rightarrow WW^*$	(ggH, VBF)
$H \rightarrow \tau\tau$	(ggH, VBF)
$H \rightarrow b\bar{b}$	(VBF)
$H \rightarrow b\bar{b}$	($t\bar{t}H$)
$H \rightarrow$ multilepton	($t\bar{t}H$)
$H \rightarrow \mu\mu$	(all production modes)

$M_h^{125}(\tilde{\chi})$ scenario



$M_{h,EFT}^{125}$ scenario



SMEFT Interpretation

- Includes full Run 2 dataset analyses with differential STXS measurements

Analysis	Integrated lumi (fb ⁻¹)
$H \rightarrow \gamma\gamma$ (all production modes)	139
$H \rightarrow ZZ^* \rightarrow 4\ell$ (all production modes)	139
$H \rightarrow b\bar{b}$ (VH)	139

- In practice, introduce set of operators to the SM Lagrangian:

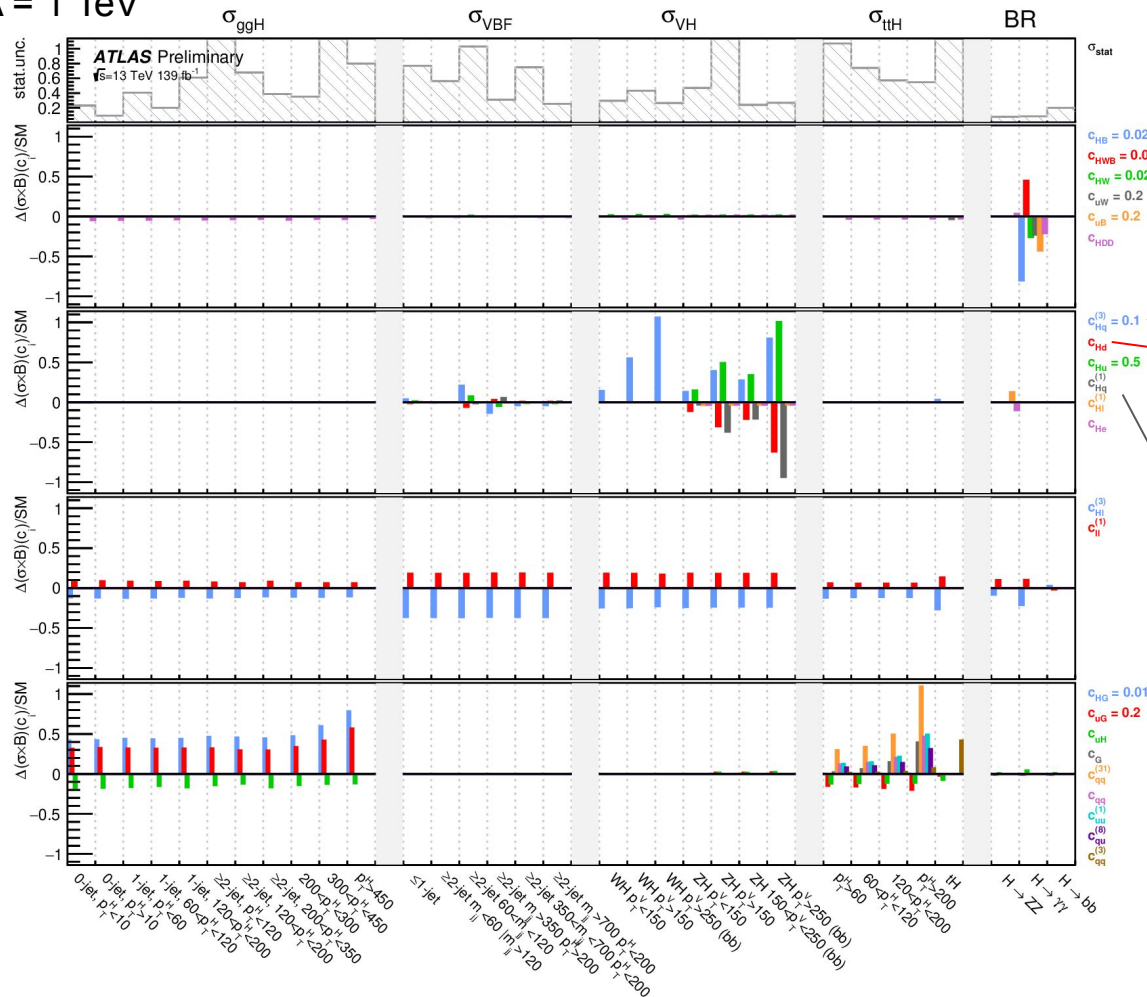
$$\mathcal{L}_{\text{SMEFT}} = \mathcal{L}_{\text{SM}} + \sum_i^{N_{d6}} \frac{c_i}{\Lambda^2} \mathcal{O}_i^{(6)} + \sum_j^{N_{d8}} \frac{b_j}{\Lambda^4} \mathcal{O}_j^{(8)} + \dots$$

Considering $\mathcal{O}_i^{(6)}$ operators, evaluate the expected effect of nonzero values of each parameter c_i on measurable Higgs kinematics, and constrain parameters based on combination of Higgs measurements

- Interpretations for linear (interference terms) and linear+quadratic (interference+pure BSM terms) dependence on d=6 SMEFT operators

$\Lambda = 1 \text{ TeV}$

SMEFT Interpretation



$(H^\dagger i \overleftrightarrow{D}_\mu^I H)(\bar{q}_p \tau^I \gamma^\mu q_r)$	
$(H^\dagger i \overleftrightarrow{D}_\mu H)(\bar{d}_p \gamma^\mu d_r)$	
$(H^\dagger i \overleftrightarrow{D}_\mu H)(\bar{u}_p \gamma^\mu u_r)$	
$(H^\dagger i \overleftrightarrow{D}_\mu H)(\bar{q}_p \gamma^\mu q_r)$	

Many parameters: for illustration, focus on a set that largely affects VH

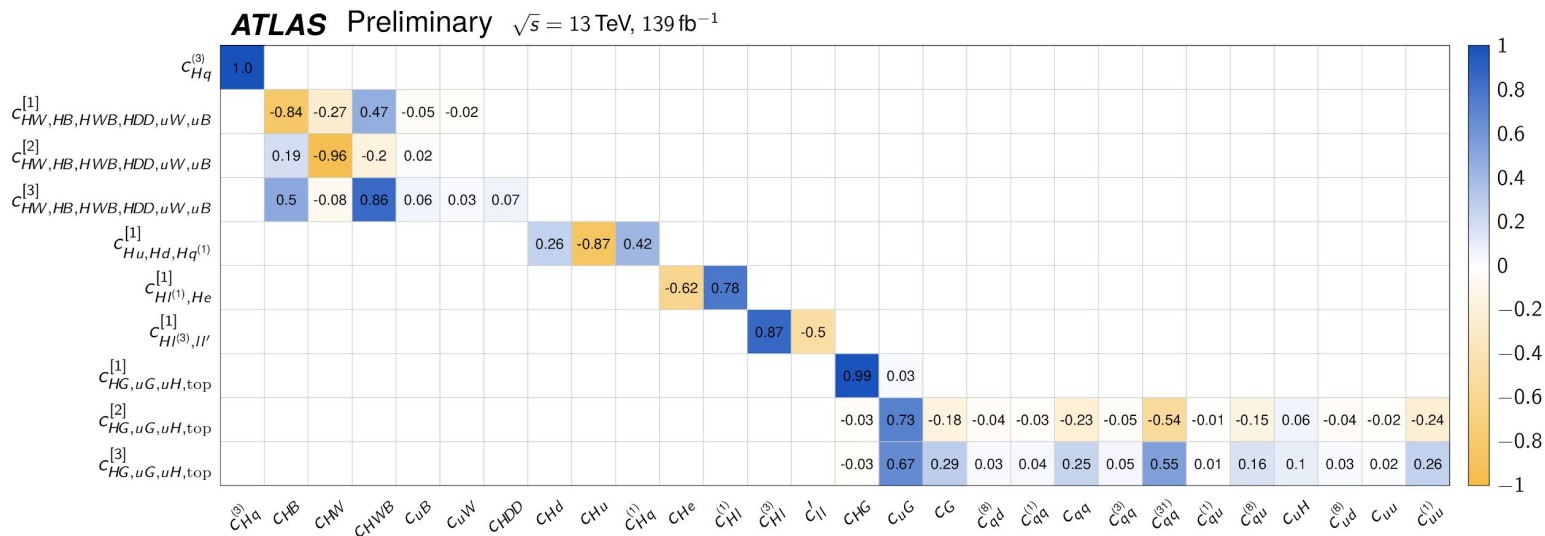
Only linear terms in model in figure: model with quadratic terms also included in result

SMEFT Interpretation

Due to large number of parameters with complicated correlation,
Cannot separately constrain all parameters

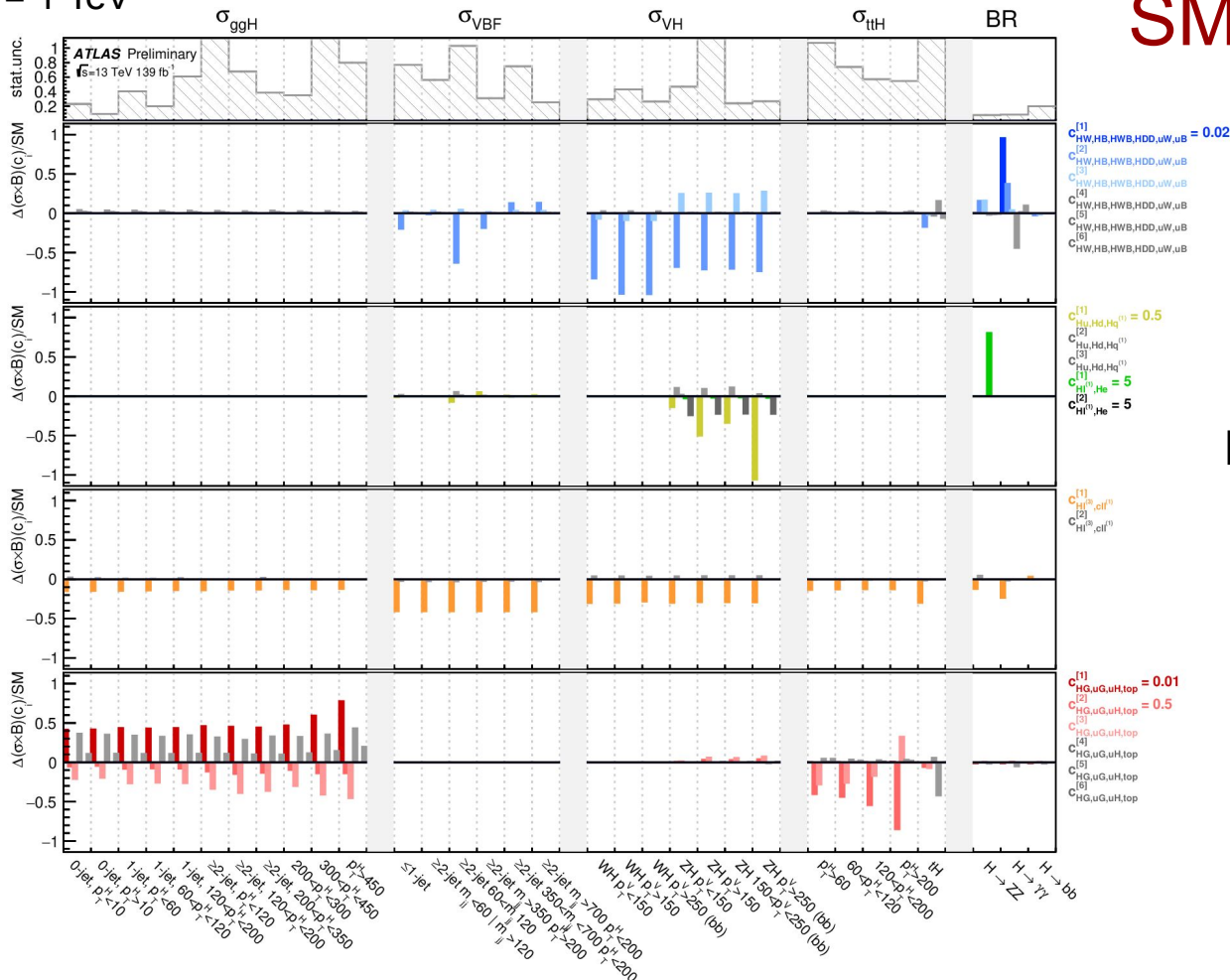
Decompose into subspaces, motivated by correlations and physics concerns

Set parameters with weak eigenvalues to 0 and fit resulting parameter set



$\Lambda = 1 \text{ TeV}$

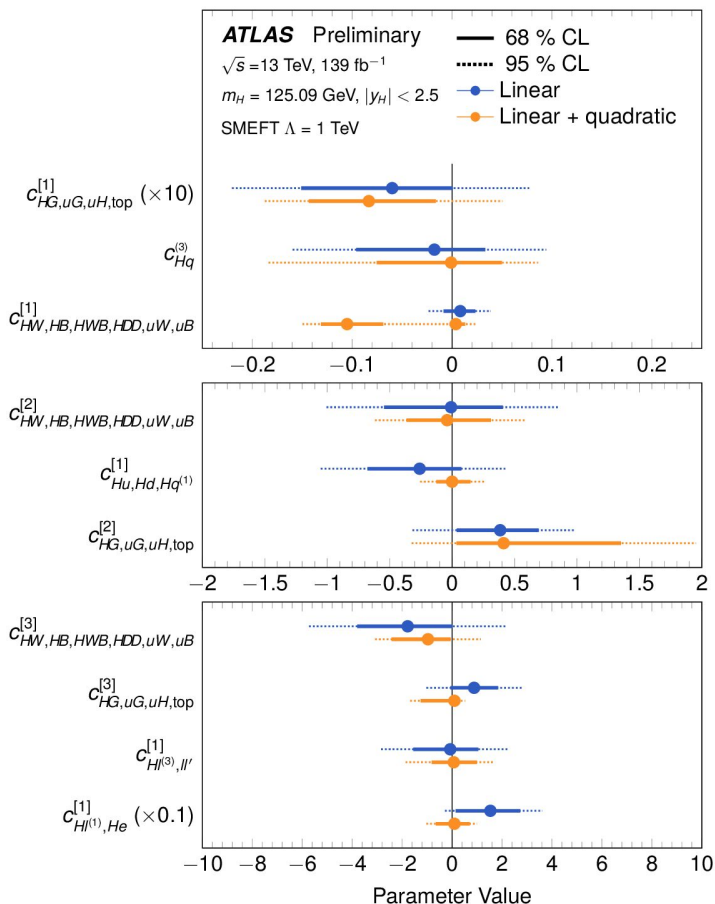
SMEFT Interpretation



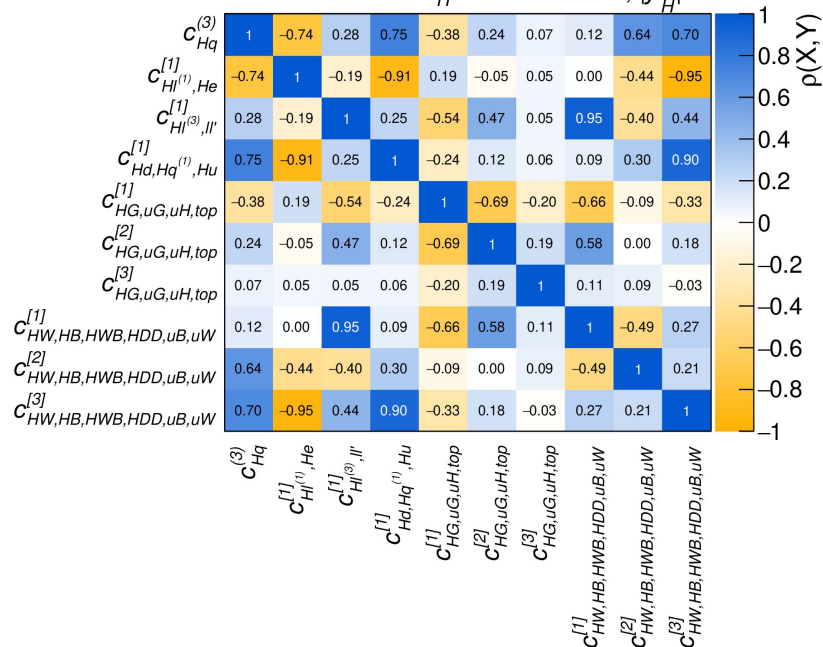
Fit resulting parameter set

SMEFT Results

Parameter measurements and correlations



ATLAS Preliminary $\sqrt{s} = 13 \text{ TeV}, 139 \text{ fb}^{-1}$
 $m_H = 125.09 \text{ GeV}, |y_H| < 2.5$



- Inclusion of quadratic terms → tighter constraints
- Suggests a non-negligible influence of $d = 6$ operator terms suppressed by power Λ^{-4}

Conclusion

New results presented for VBF and ttH(bb)
→expect $\sim 3\sigma$ for both

For VBF, measured 3σ for $H\rightarrow bb$ production

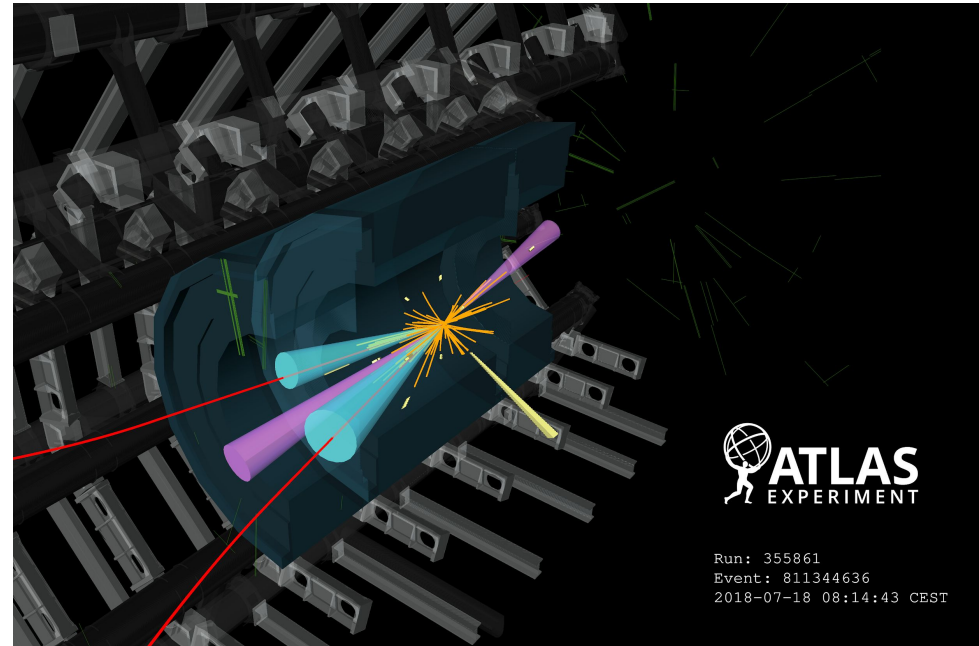
For ttH, performed differential p_T^H measurement up to highest ever p_T^H values for ttH

For ttH, many improvements possible, particularly with improved understanding of background modeling

ggF $H\rightarrow bb$ with full Run 2 dataset is still in progress

New ATLAS combinations, make new interpretations in MSSM and SMEFT scenarios

Updated already-precise $H\rightarrow inv$ limits through combination with previous and reinterpreted results



Candidate VBF+ γ event

Backup

Citations

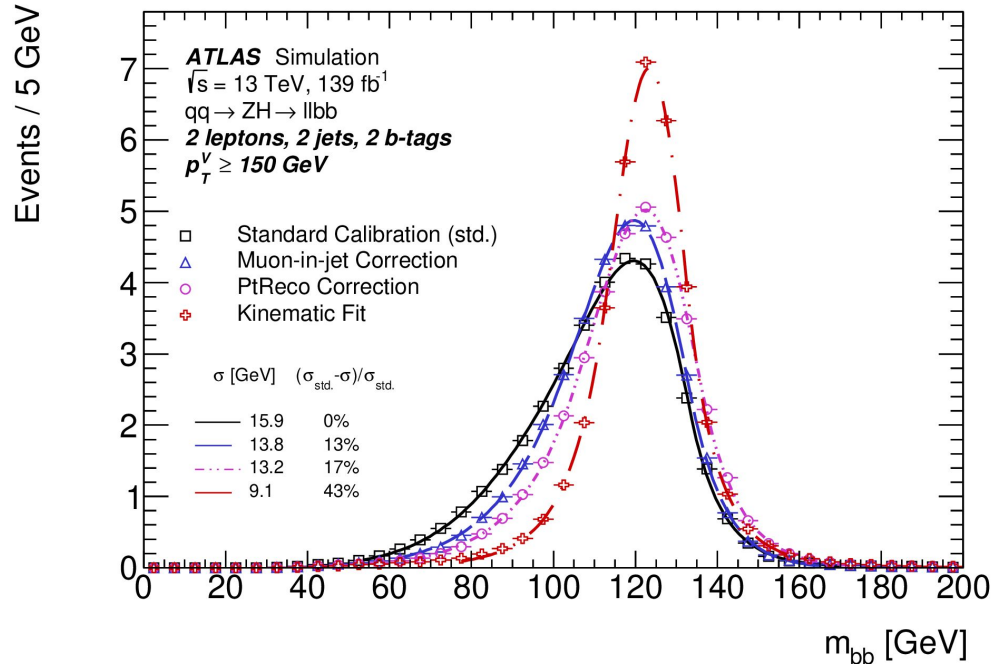
Gabrielli, E., Mele, B., Piccinini, F. *et al.* Asking for an extra photon in Higgs production at the LHC and beyond. *J. High Energ. Phys.* 2016, 3 (2016)

A. D. Bukin, Fitting function for asymmetric peaks, 2007, arXiv: 0711.4449 [physics.data-an]

B-jet Corrections

m_{bb} resolution using different b-jet corrections

VBF and VBF+ γ use **muon-in-jet** and **PtReco**

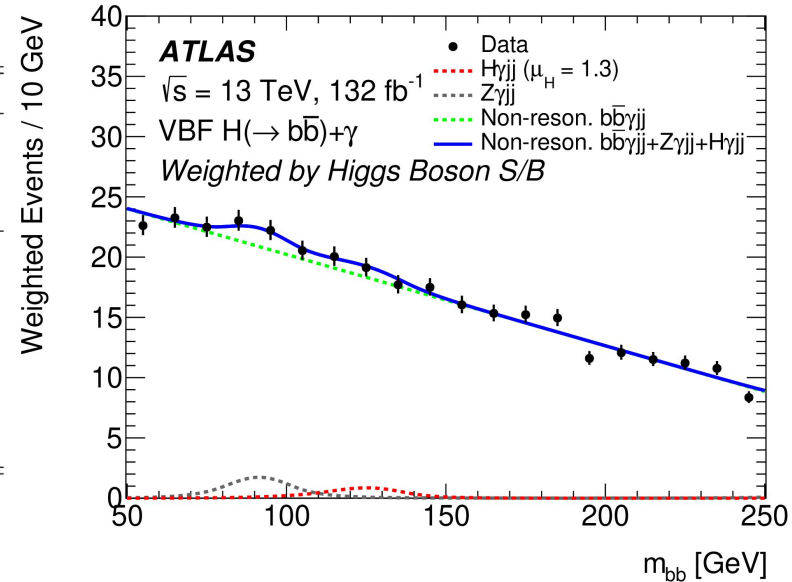


VBF+ γ : Selection and results

Left: Full event preselection

Right: weighted sum of signal regions, including non-resonant background

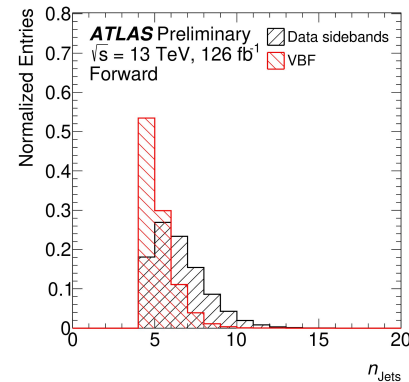
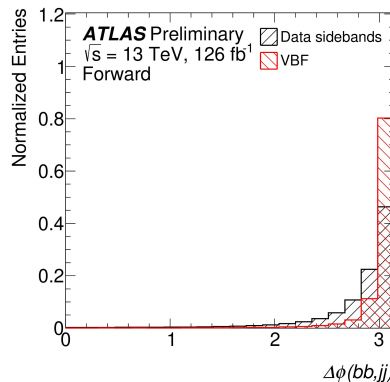
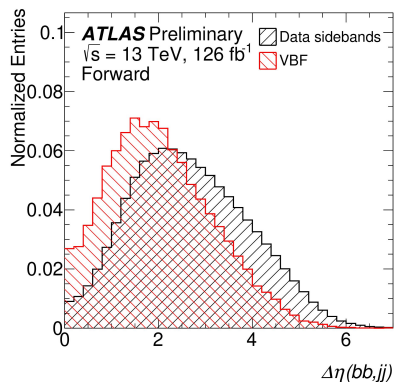
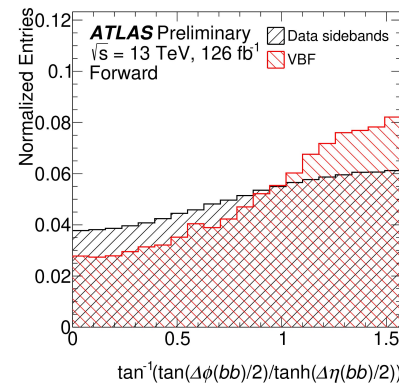
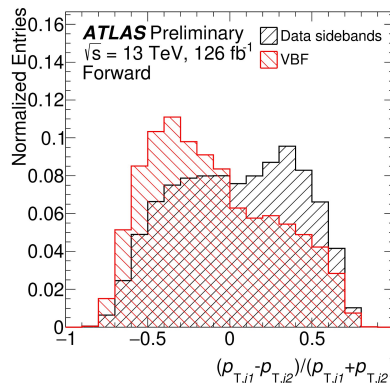
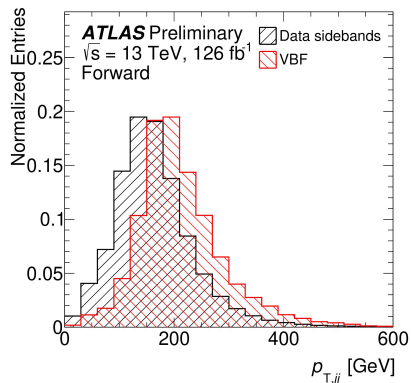
Trigger	L1	≥ 1 photon with $E_T > 22$ GeV
	HLT	≥ 1 photon with $E_T > 25$ GeV ≥ 4 jets (or ≥ 3 jets and ≥ 1 b -jet) with $E_T > 35$ GeV and $ \eta < 4.9$ $m_{jj} > 700$ GeV
Offline		≥ 1 photon with $E_T > 30$ GeV and $ \eta < 1.37$ or $1.52 < \eta < 2.37$ ≥ 2 b -jets with $p_T > 40$ GeV and $ \eta < 2.5$ ≥ 2 jets with $p_T > 40$ GeV and $ \eta < 4.5$ $m_{jj} > 800$ GeV $p_T(b\bar{b}) > 60$ GeV No electrons ($p_T > 25$ GeV, $ \eta < 2.47$) or muons ($p_T > 25$ GeV, $ \eta < 2.5$)



All-hadronic VBF $H \rightarrow bb$ Variable List

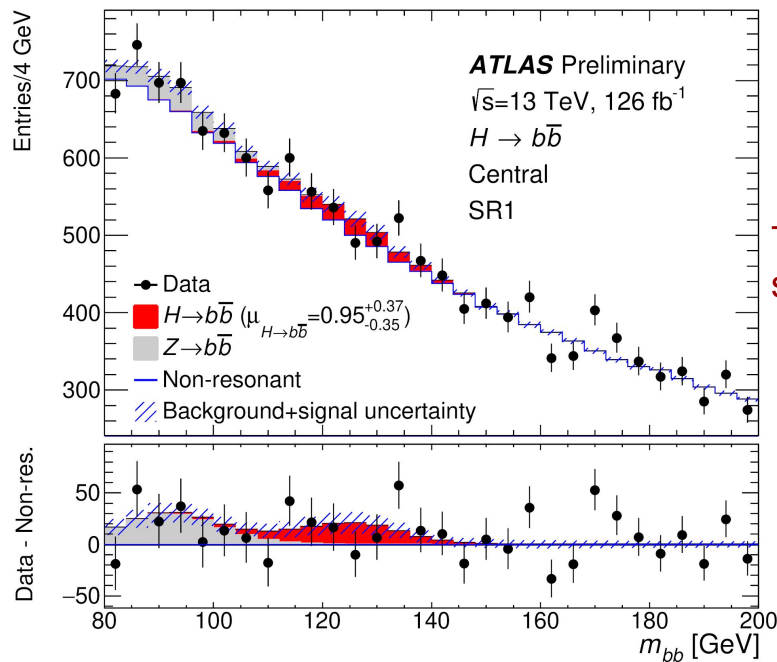
11 (12) input variables for Forward (Central) channel. In the Forward channel, N_{trk}^{j1} is not included, as one of the jets is always in the forward region and has no associated tracks

- m_{jj}
- $p_{T,jj}$
- p_T balance
- $\Delta\eta(bb,jj)$
- $\Delta\phi(bb,jj)$
- N jets
- $(p_T^{j1} - p_T^{j2}) / (p_T^{j1} + p_T^{j2})$
- $\tan^{-1}(\tan(\frac{1}{2}\Delta\phi^{bb}) / \tanh(\frac{1}{2}\Delta\eta^{bb}))$
- $N_{\text{trk}}^{j1(2)}$ (q/g tagging)
- $\min(\Delta R(j^{1(2)}, \text{extra jet}))$

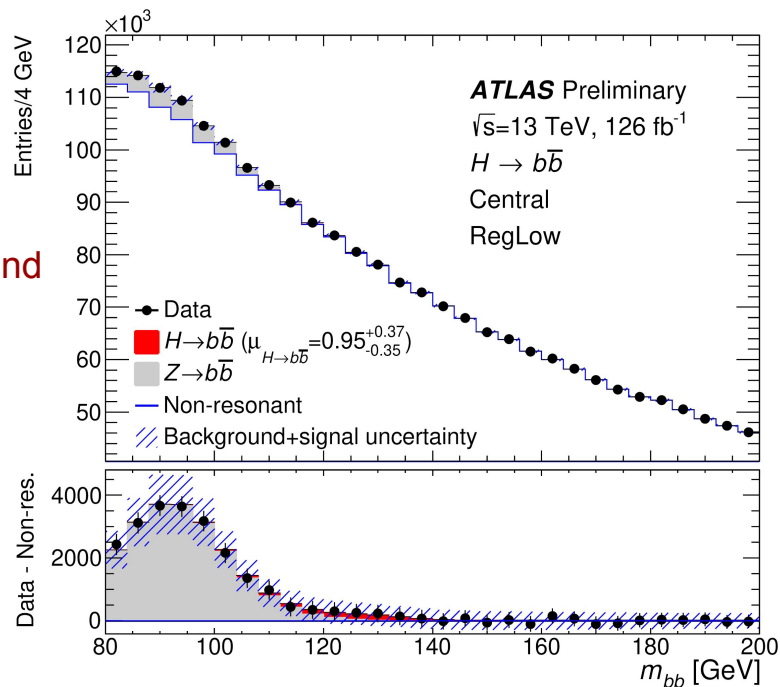


Fits (Central Channel)

- Score and m_{bb} uncorrelated \rightarrow take background template in high score signal regions from high-statistic low score control region
- Fit 4 high score regions + one low score region in each channel (10 regions total)

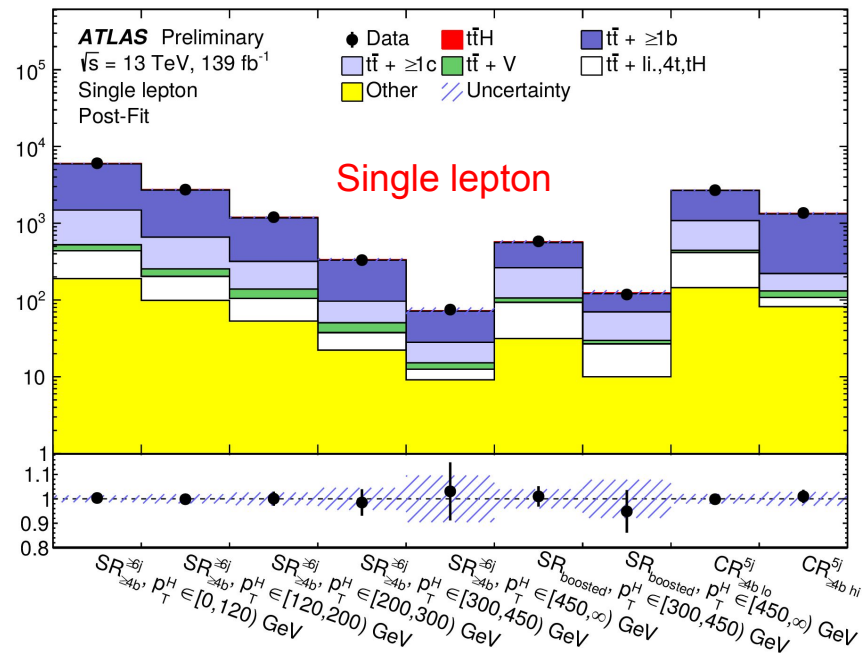
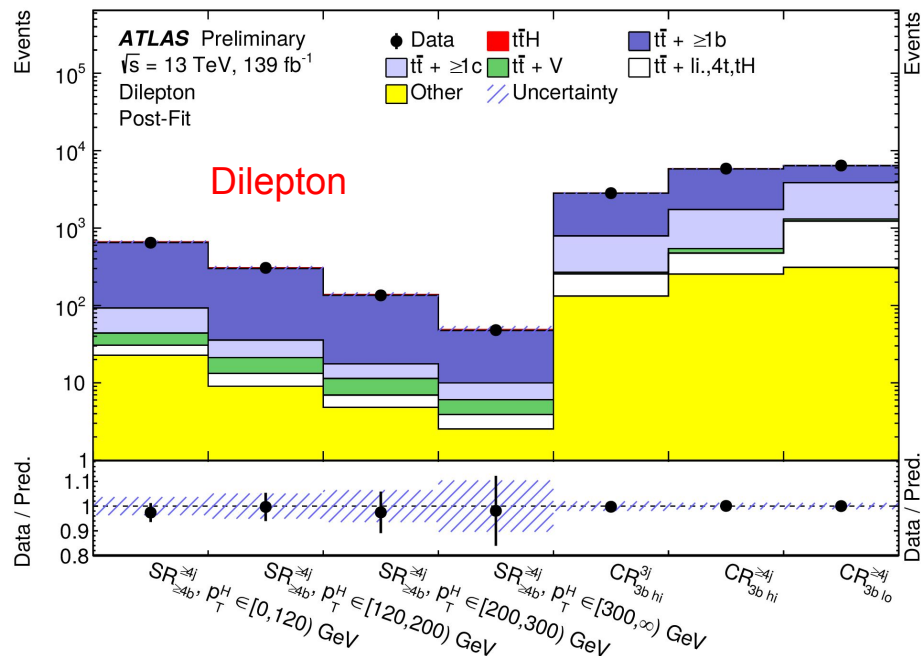


Take background shape from



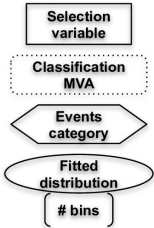
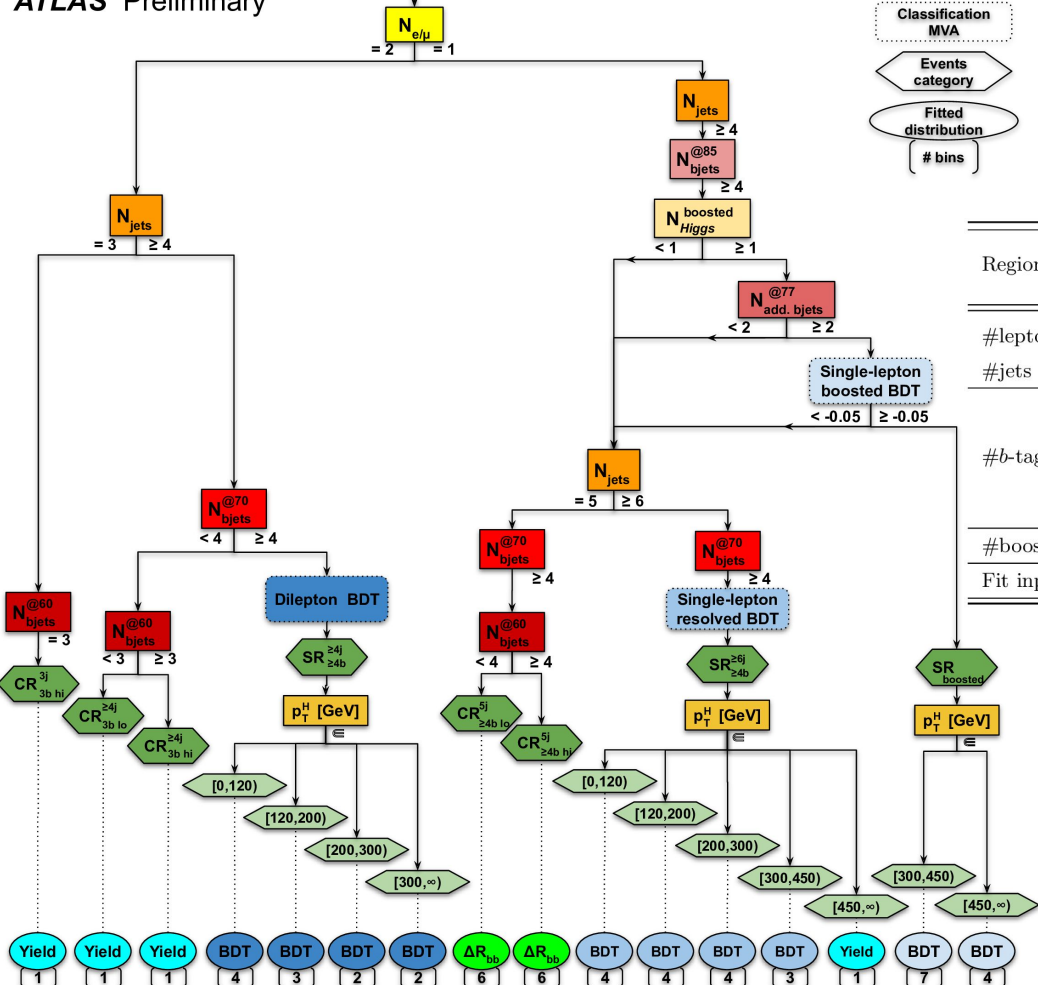
ttH Post-fit Channels

Event yields in each SR and CR, post-fit



Events after trigger, object selection and overlap removal, Z veto

ATLAS Preliminary



Classification Flowchart

Schematic view of all channels and regions in the analysis

Region	Dilepton				Single-lepton			
	$SR_{\geq 4b}^{\geq 4j}$	$CR_{3b\ hi}^{\geq 4j}$	$CR_{3b\ lo}^{\geq 4j}$	$CR_{3b\ hi}^{3j}$	$SR_{\geq 4b}^{\geq 6j}$	$CR_{\geq 4b\ hi}^{5j}$	$CR_{\geq 4b\ lo}^{5j}$	SR_{boosted}
#leptons	= 2				= 1			
#jets	≥ 4		= 3		≥ 6	= 5		≥ 4
@85%	-				≥ 4			
@77%	-				-			≥ 2 [†]
@70%	≥ 4	= 3		= 3	≥ 4		-	
@60%	-	= 3	< 3	= 3	-	≥ 4	< 4	-
#boosted cand.	-				0		≥ 1	
Fit input	BDT		Yield		BDT/Yield		$\Delta R_{bb}^{\text{avg}}$	BDT

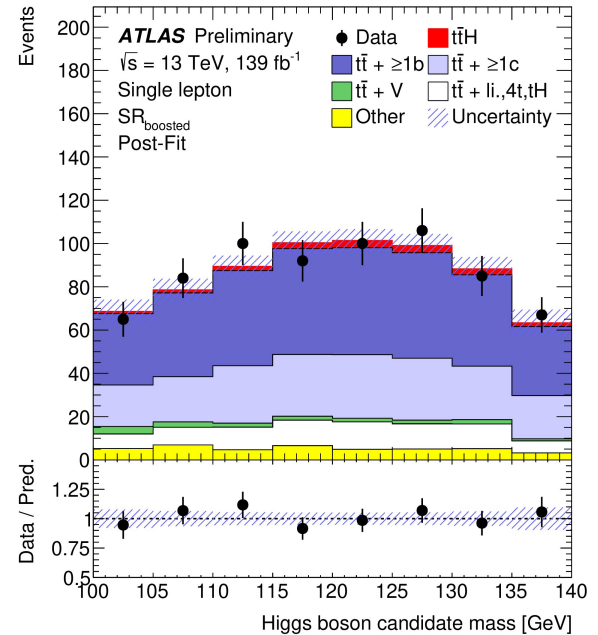
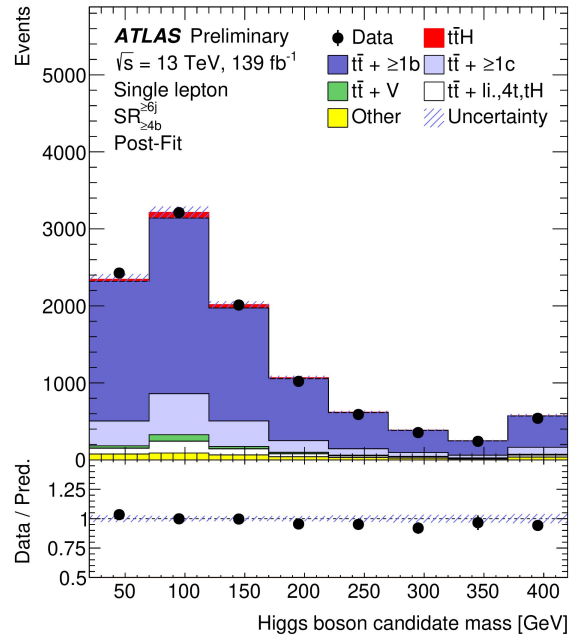
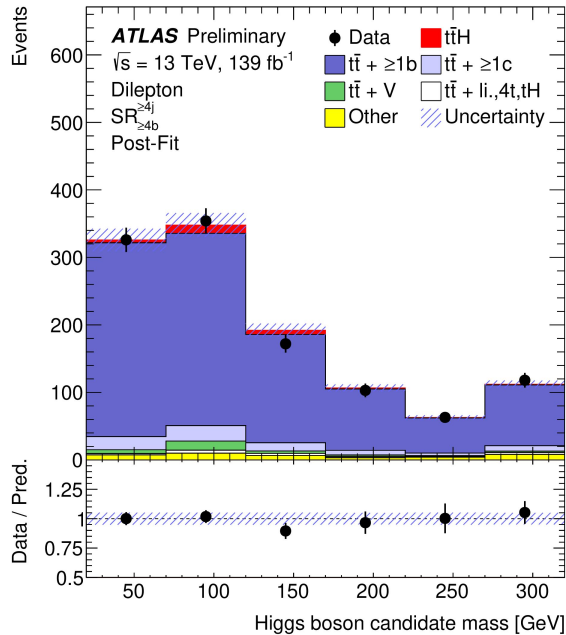
ttH Uncertainties

Uncertainty source	$\Delta\mu$	
$t\bar{t} + \geq 1b$ modelling	+0.25	-0.24
$t\bar{t}H$ modelling	+0.14	-0.06
tW modelling	+0.08	-0.08
b -tagging efficiency and mis-tag rates	+0.05	-0.05
Background-model statistical uncertainty	+0.05	-0.05
Jet energy scale and resolution	+0.03	-0.03
$t\bar{t} + \geq 1c$ modelling	+0.03	-0.03
$t\bar{t} + \text{light}$ modelling	+0.02	-0.02
Luminosity	+0.01	-0.00
Other sources	+0.03	-0.03
Total systematic uncertainty	+0.30	-0.27
$t\bar{t} + \geq 1b$ normalisation	+0.03	-0.05
Total statistical uncertainty	+0.20	-0.19
Total uncertainty	+0.36	-0.33

Summary of uncertainties, broken down by source

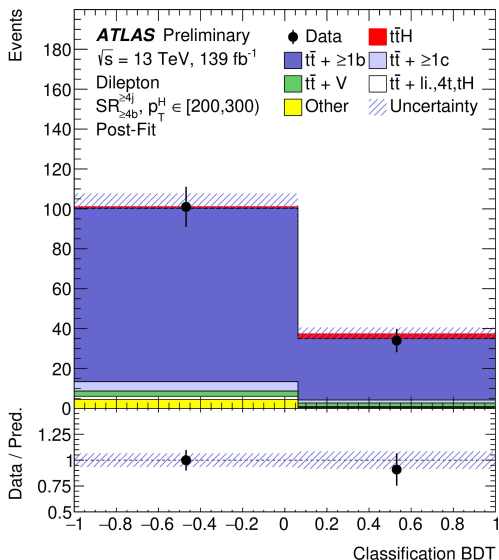
ttH: m_{bb} Distributions

Mass distributions in each analysis channel

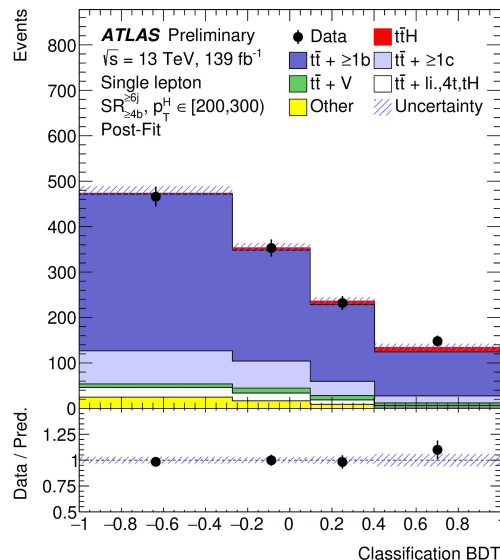


Example: $200 < p_T^H < 300$ GeV

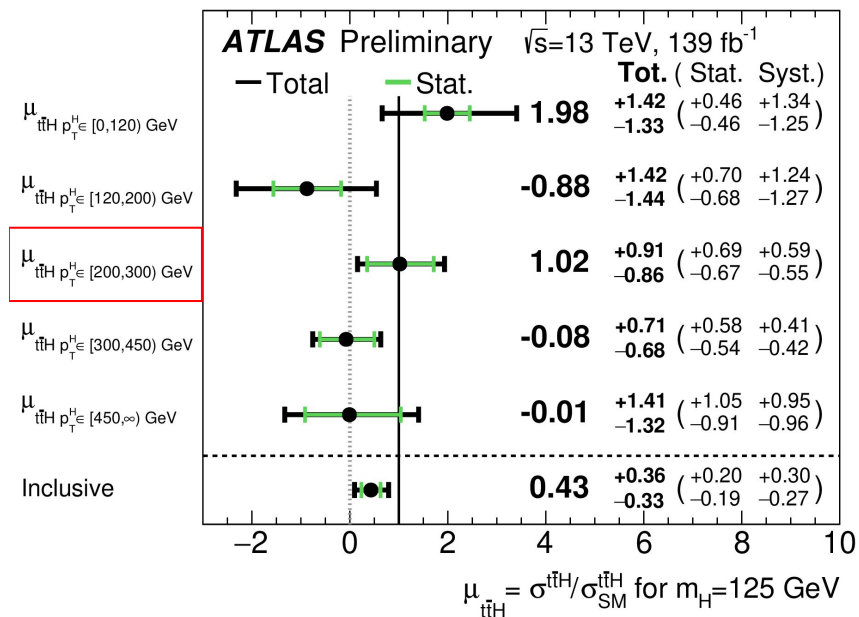
- As example, results from fit for 200-300 GeV bin shown, which generally constrain the signal-strength for $200 < p_T^H < 300$ GeV
- Table gives measured signal-strength in all p_T^H bins



Dilepton

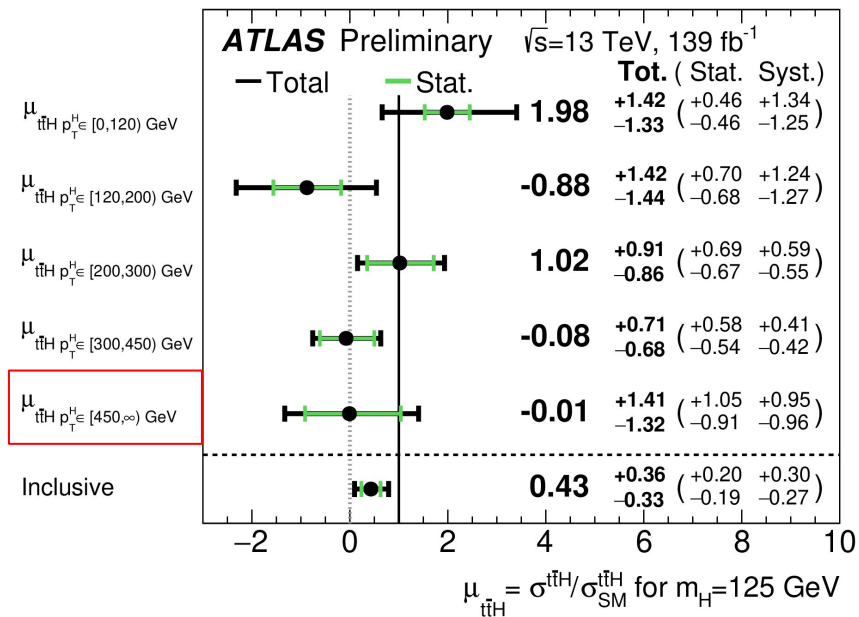
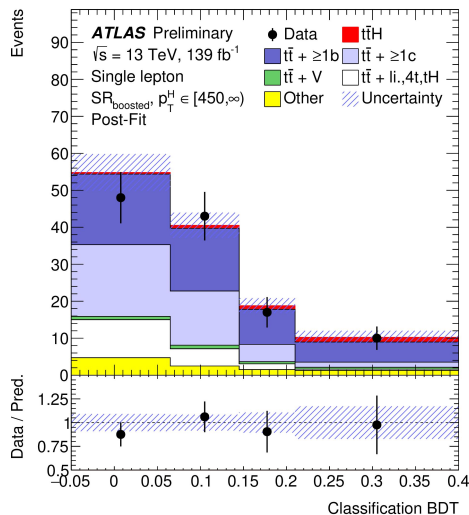
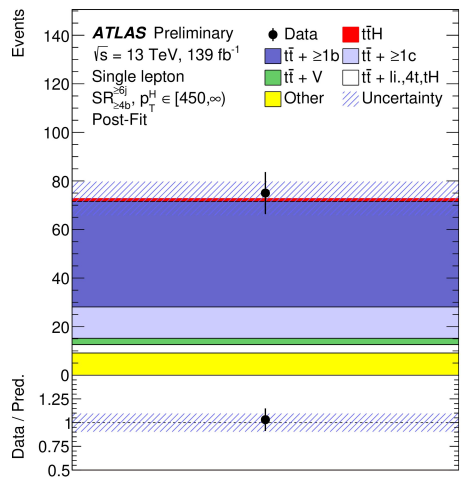
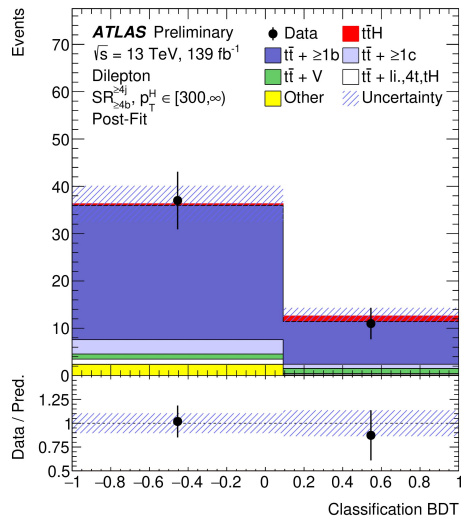


Single lepton



Results: $p_T^H > 450$ GeV

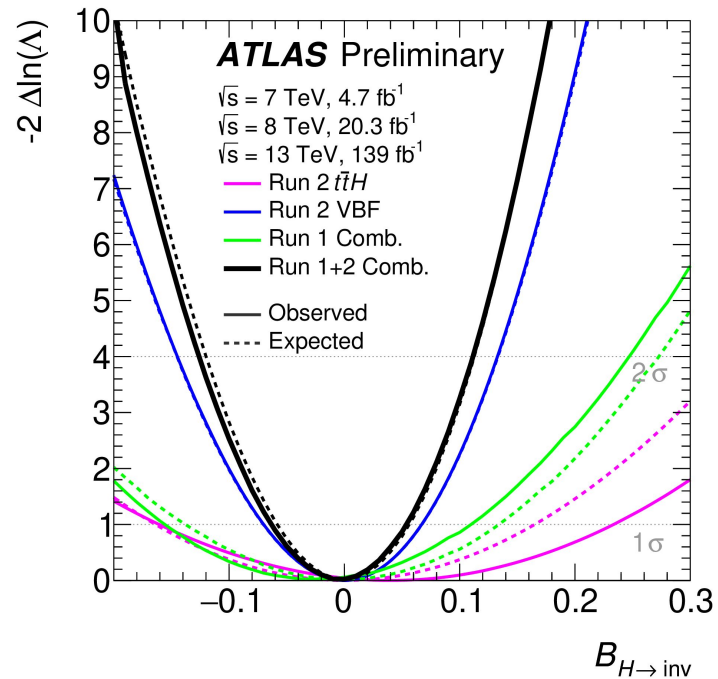
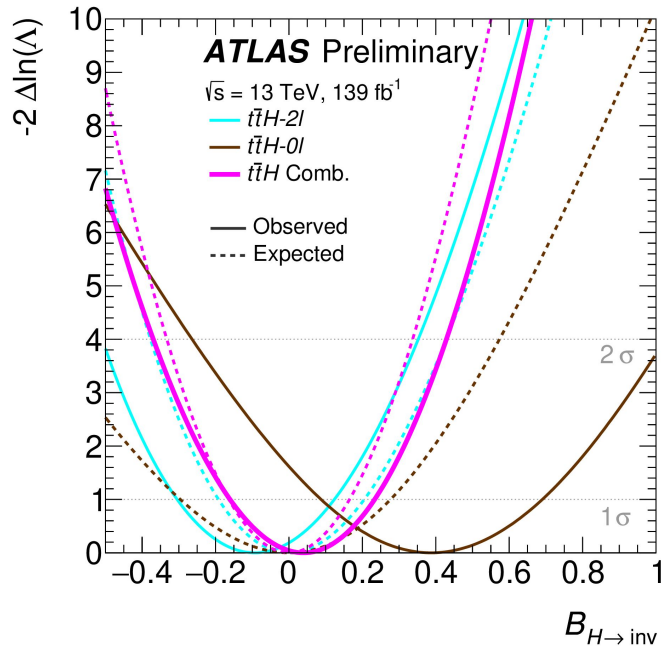
- Results shown for $p_T^H > 450$ GeV bin for 1-lepton channels and $p_T^H > 300$ GeV bin for 2-lepton channel



H→invisible: ttH and Expectations

Left: Results from individual ttH analyses

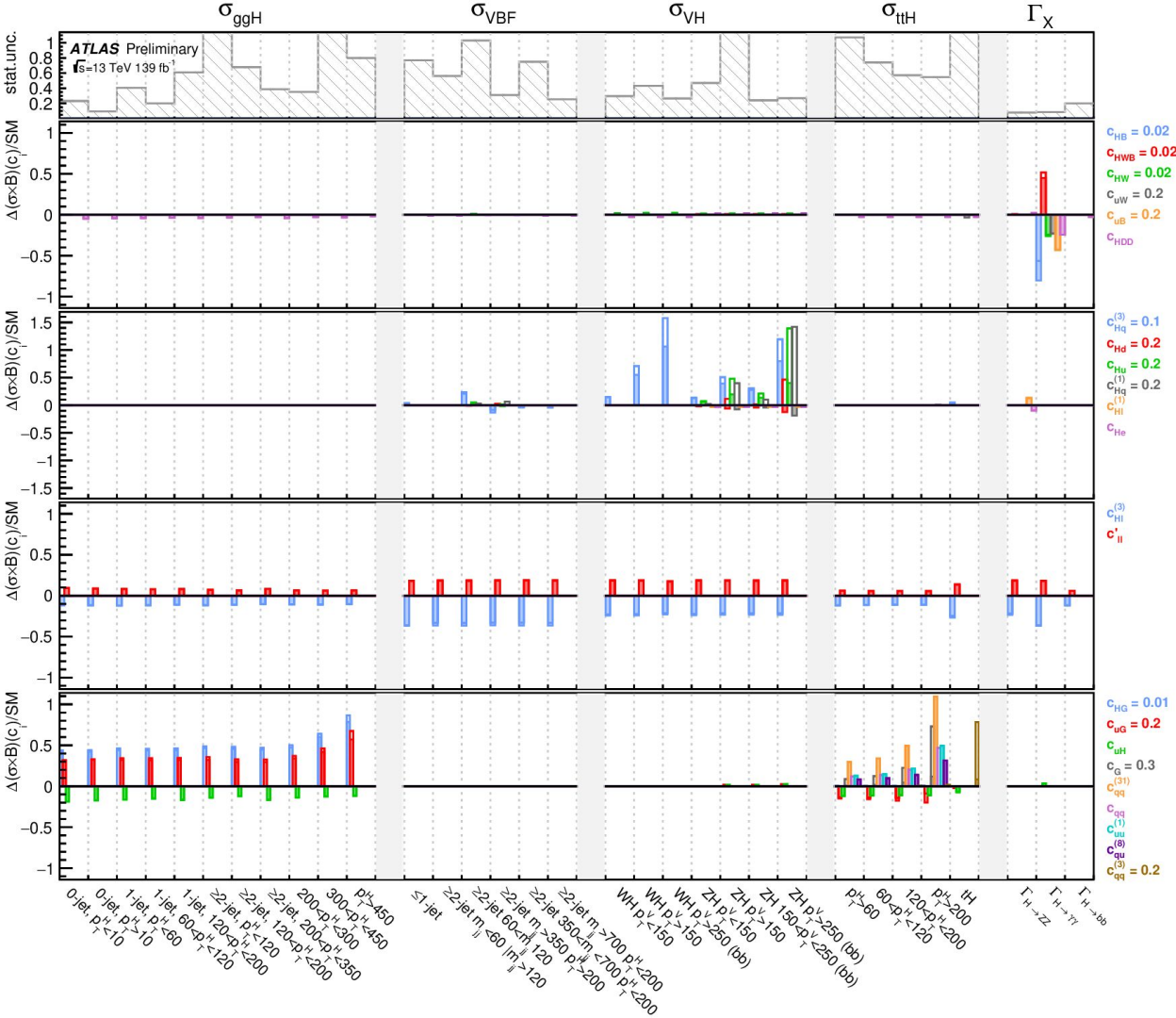
Right: Results for each channel, showing both observation and expectation



H→invisible: Uncertainties

Source of uncertainty	±Uncertainty on $\mathcal{B}_{H\rightarrow\text{inv}}$	
	Run 2	Run 1+2
Luminosity / pile up	0.002	0.003
Leptons / photons	0.018	0.015
Jets	0.023	0.019
Flavour tagging	0.002	0.002
E_T^{miss}	0.008	0.007
V+jets modelling	0.011	0.017
Other background modelling	0.015	0.015
Data-driven background	0.023	0.019
Signal modelling	0.004	0.003
MC statistics	0.023	0.021
All experimental	0.041	0.036
All theory	0.030	0.030
Total systematic uncertainty	0.051	0.046
Data statistics	0.019	0.018
Floating background norm.	0.031	0.028
Total statistical uncertainty	0.037	0.034
Total uncertainty	0.063	0.057

Source of uncertainty	±Uncertainty on $\mathcal{B}_{H\rightarrow\text{inv}}$
	$t\bar{t}H$
Luminosity / pile up	0.006
Leptons / photons	0.025
Jets	0.036
Flavour tagging	0.019
E_T^{miss}	0.013
$t\bar{t}$ modelling	0.055
$t\bar{t} + Z$ modelling	0.035
Other background modelling	0.047
Data-driven background	0.003
Signal modelling	0.015
MC statistics	0.009
All experimental	0.053
All theory	0.080
Total systematic uncertainty	0.099
Data statistics	0.116
Floating background norm.	0.064
Total statistical uncertainty	0.132
Total uncertainty	0.165



Linear+Quadratic Model

Impact of each parameter, showing both linear (shaded) and linear+quadratic (open) models

MSSM Interpretation Summary

Overview of benchmark models:

- M_h^{125} :
 - All superparticles heavy that production → MSSM Higgs bosons only mildly affected by them.
 - Heavy Higgs bosons with masses up to 2 TeV decay only to SM particles.
- $M_h^{125}(X\tilde{~})$:
 - All charginos and neutralinos relatively light, with significant higgsino-gaugino mixing.
 - Weakens exclusion bounds from $H/A \rightarrow \tau\tau$ searches, as well as the decay of the SM-like Higgs boson to photons.
 - Possibility to look for additional Higgs bosons through their decays to charginos and neutralinos opens up.
- $M_h^{125}(\tau\tilde{~})$ scenario:
 - Light staus and light gaugino-like charginos and neutralinos.
 - The effect of the light staus on the decays of the heavier Higgs bosons, as well as on the decay of the SM-like Higgs boson to photons, is most relevant at large $\tan\beta$.
 - Compared with the previous scenario, a larger mass for the higgsinos implies that the decays of the heavier Higgs bosons to charginos and neutralinos become relevant at larger values of M_A .
- M_h^{125} (alignment) scenario:
 - In the “alignment without decoupling” scenario, for a given value of $\tan\beta$, one of the two neutral CP-even scalars has SM-like couplings independently of the mass spectrum of the remaining Higgs bosons.
 - In particular, for $\tan\beta$ around 7 the properties of the lighter scalar h are in agreement with those of the observed Higgs boson also for relatively low values of M_A .

MSSM Interpretation Summary

Overview of benchmark models:

- $M_{h,EFT}^{125}$:
 - Characterized by a flexible mass scale M_{SUSY} of the superpartners.
 - The parameter region $\tan \beta < 5$ is ruled out because the mass M_h of the SM-like Higgs boson is predicted to be lower than the measured value.
 - To re-open the parameter region of low $\tan \beta$ values, the sfermion mass scale, M_{SUSY} is adjusted dynamically from 6 TeV to 10^{16} TeV to achieve a 125 GeV Higgs.
 - As in this scenario all superparticles are chosen to be so heavy that production and decays of the MSSM Higgs bosons are only mildly affected by their presence, the SUSY contribution to the Higgs properties is calculated with an effective field theory (EFT).
- $M_{h,EFT}^{125}(\tilde{\chi})$ scenario:
 - Features light neutralinos and charginos whose presence significantly alters the phenomenology of the Higgs boson.
 - The SUSY scale is again adjusted at every parameter point in order to obtain a light Higgs mass of $M_h \approx 125$ GeV.

MSSM Interpretation Summary

